

FOXP3⁺ Regulatory T Cells Affect the Development and Progression of Hepatocarcinogenesis

Noritoshi Kobayashi,¹ Nobuyoshi Hiraoka,¹ Wataru Yamagami,¹ Hidenori Ojima,¹ Yae Kanai,¹ Tomoo Kosuge,² Atsushi Nakajima,³ and Setsuo Hirohashi¹

Abstract Purpose: Tumor-infiltrating lymphocytes represent the host immune response to cancer. CD4⁺CD25⁺FOXP3⁺ regulatory T cells (Tregs) suppress the immune reaction. The aim of the present study was to investigate the clinicopathologic significance and roles of Tregs and CD8⁺ T cells during hepatocarcinogenesis.

Experimental Design: We examined the infiltration of FOXP3⁺ Tregs and CD8⁺ T cells in the tumor stroma and nontumorous liver parenchyma using 323 hepatic nodules including precursor lesions, early hepatocellular carcinoma (HCC), and advanced HCC, along with 39 intrahepatic cholangiocarcinomas and 59 metastatic liver adenocarcinomas. We did immunohistochemical comparative studies.

Results: The prevalence of Tregs was significantly higher in HCC than in the nontumorous liver ($P < 0.001$). The patient group with a high prevalence of Tregs infiltrating HCC showed a significantly lower survival rate ($P = 0.007$). Multivariate analysis revealed that the prevalence of Tregs infiltrating HCC was an independent prognostic factor. The prevalence of Tregs increased in a stepwise manner ($P < 0.001$) and that of CD8⁺ T cells decreased during the progression of hepatocarcinogenesis ($P < 0.001$). Regardless of the presence of hepatitis virus infection or histopathologic evidence of hepatitis, the prevalence of Tregs was significantly increased in nontumorous liver bearing primary hepatic tumors.

Conclusions: Tregs play a role in controlling the immune response to HCC during the progression of hepatocarcinogenesis. It has been suggested that primary hepatic cancers develop in liver that is immunosuppressed by a marked infiltration of Tregs. A high prevalence of Tregs infiltrating HCC is thought to be an unfavorable prognostic indicator.

Hepatocellular carcinoma (HCC) is the fifth most common cancer in the world, representing the third most common cause of mortality among deaths from cancer (1). Even with remarkable advances in diagnostic and therapeutic techniques, the incidence of HCC is still on the increase. Hepatitis virus B (HBV) and hepatitis virus C (HCV) are known to be major risk factors, and chronic infection with these viruses is responsible for ~80% of HCCs in humans (2). Most of the HCCs occur

in damaged liver (chronic hepatitis or liver cirrhosis), even if the liver is not infected with HBV or HCV (3). HCC is also characterized by an obvious multistage process of tumor progression (4–7), from a regenerative nodule to adenomatous hyperplasia (AH), and thereafter to atypical adenomatous hyperplasia (AAH), early HCC (defined as *in situ* or micro-invasive cancer), and advanced HCC. It is important to detect cancers at an early stage, including their precursor lesions, and to assess their risk in order to provide appropriate treatment and reduce cancer-related mortality.

Previous studies have investigated the changes in morphology, genetics, and molecular biology of epithelial cells during tumorigenesis. Recently, many studies have suggested that the tumor microenvironment also plays an important role in the establishment and progression of tumors. Lymphocytes contribute to the tumor microenvironment through immunity and inflammation. CD8⁺ CTLs can directly kill target cells by releasing granules including membrane-lytic materials such as perforin and granzymes in acquired immune responses, thereby playing a central role in antitumor immunity. Indeed, a high frequency of CD8⁺ T cells infiltrating cancer tissue can be a favorable prognostic indicator in ovarian cancer (8) and colorectal cancer (9). In HCC, extremely marked infiltration of T cells including predominant CD8⁺ T cells has been shown to be closely associated with a low recurrence rate and good prognosis (10). On the other hand, another study using a mouse model has

Authors' Affiliations: ¹Pathology Division, National Cancer Center Research Institute; ²Division of Hepato-Biliary and Pancreatic Surgery, National Cancer Center Hospital, Tokyo, Japan; and ³Gastroenterology Division, Yokohama City University Hospital, Yokohama, Japan

Received 9/25/06; revised 10/29/06; accepted 11/8/06.

Grant support: Grant-in-Aid for Third Term Comprehensive 10-year Strategy for Cancer Control from the Ministry of Health, Labor, and Welfare of Japan and a Grant-in-Aid for Scientific Research from the Ministry of Education, Culture, Sports, Science, and Technology of Japan. N. Kobayashi and W. Yamagami are recipients of a Research Resident Fellowship from the Foundation for Promotion of Cancer Research in Japan.

The costs of publication of this article were defrayed in part by the payment of page charges. This article must therefore be hereby marked *advertisement* in accordance with 18 U.S.C. Section 1734 solely to indicate this fact.

Requests for reprints: Nobuyoshi Hiraoka, Pathology Division, National Cancer Center Research Institute, 5-1-1 Tsukiji, Chuo-ku, Tokyo 104-0045, Japan. Phone: 81-33542-2511; Fax: 81-33248-2463; E-mail: nhiraoka@gan2.res.ncc.go.jp.

© 2007 American Association for Cancer Research.
doi:10.1158/1078-0432.CCR-06-2363

shown that marked infiltration of CD8⁺ T cells exacerbates liver damage, thus accelerating the development of HCC (11).

In contrast to CD8⁺ CTL, which generally exert a suppressive influence on tumor growth, regulatory T cells (Tregs) are thought to have a positive effect on tumor growth through suppression of antitumor immune cells. CD4⁺CD25⁺ Tregs are a minor but functionally unique population of T cells, which maintain immune homeostasis in immune tolerance and the control of autoimmunity. Tregs can inhibit immune responses mediated by CD4⁺CD25⁻ and CD8⁺ T cells *in vitro* by a contact-dependent and cytokine-independent mechanism (12–14), although more recent reports suggest that the immune suppression mechanisms of Tregs *in vivo* are more complex (15, 16). Forkhead or winged helix family of transcription factor P3 (FOXP3) is critical for the development and function of Tregs in mice and humans (16, 17), and is still the only marker for evaluating real Tregs that have a suppressive function. In murine models, it has been described that Tregs inhibit the antitumor immune response (15, 18–20). Involvement of CD4⁺CD25⁺ Tregs in human cancer has been observed in peripheral blood and tumor tissues from patients with several types of cancer (21–25). A few groups have reported that Tregs are increased in peripheral blood and among tumor-infiltrating lymphocytes of patients with HCC (26–28), although these were not large-scale studies and did not estimate the clinicopathologic significance of Tregs infiltrating HCC, including their prognostic value. Early studies detected Tregs not as FOXP3⁺ T cells but as CD4⁺CD25⁺ T cells, although recent studies have revealed that CD4⁺CD25⁺ T cells consist of Tregs and activated effector T cells, the latter being increased in inflammatory lesions (29). Furthermore, no previous study has investigated host immune responses in multistage hepatocarcinogenesis.

In the present study, we first investigated the clinicopathologic values of both FOXP3⁺ Tregs and CD8⁺ T cells infiltrating the tumor stroma of HCC, and then examined the prevalence of FOXP3⁺ Tregs and CD8⁺ T cells during multistage hepatocarcinogenesis. Precursor lesions of HCC are small nodular lesions that can be detected and evaluated only by microscopic analysis, making it difficult to extract living immune cells from them and to analyze their immunophenotypes and immune functions. Therefore, we selected an immunohistochemical comparative approach for evaluating host immune responses in these HCC precursor lesions. This approach was used in the other experiments as well. We also investigated whether Tregs are involved in the development of HCC, and compared the host immune responses by measuring and comparing the infiltration of Tregs and CD8⁺ T cells between HCC and primary hepatic adenocarcinoma, intrahepatic cholangiocarcinoma (ICC) as well as between primary and metastatic liver tumors. We compared the prevalence of Tregs in nontumorous liver parenchyma among patients with and without primary hepatic tumors, and those with and without hepatitis viral infection. The results showed that the prevalence of Tregs increases during the progression of established cancers as well as that of their precursor lesions. Furthermore, the prevalence of Tregs was significantly correlated with patient survival, independent of other prognostic factors.

Materials and Methods

Patients and samples. This study was approved by the Ethics Committee of the National Cancer Center, Tokyo, Japan. Clinical and

pathologic data and the specimens used for immunohistochemical analysis were obtained through a detailed retrospective review of the medical records of 218 patients with 323 hepatic nodules of HCC or its precursor lesions who had undergone initial surgical resection between 1992 and 2000 at the National Cancer Center Hospital, Tokyo, Japan. None of the nodules had been treated previously with techniques such as radiofrequency ablation, percutaneous ethanol injection therapy, or transcatheter arterial embolization or injection, and none of the patients with nodules had received systemic chemotherapy. Sixty-five patients had hepatic cancers that had been treated by surgical resection, radiofrequency ablation, percutaneous ethanol injection therapy, or transcatheter arterial embolization or injection; the current nodules were also located in different lobes, as well as distant from, the previous cancers. In another six patients, curative resection was not done. The remaining 147 patients were studied in order to evaluate the clinicopathologic correlation of the prevalence of FOXP3⁺ Tregs and CD8⁺ T cells with specific variables. Tumors were classified according to the WHO classification (30) and the International Union against Cancer tumor-node-metastasis (TNM) classification (31). If patients had multiple nodules in the liver, we selected the nodule showing the most advanced histologic grade for our study. If a tumor had different grades of histology, the grade of the tumor was regarded as the most advanced one among them. Nontumorous liver was classified histopathologically into four categories: non-chronic hepatitis (NCH), chronic hepatitis (CH), chronic hepatitis with cirrhotic change (pre-cirrhotic stage; PC), and liver cirrhosis (LC), which corresponded to 0, 1-3, 4-5, and 6 of the fibrosis stages of the modified histological activity index system (32). There were 5 patients with HBV infection and 15 patients without HBV or HCV infection in NCH, which included liver with fatty changes and/or slight inflammatory infiltrates in the portal area. All patients had complete medical records and had been followed by the tumor registries for survival and outcome. Follow-up was available in all cases and ranged from 0.5 to 169.1 months (mean, 52.8 months). The latest survival data were collected on April 30, 2006. The overall survival rate at 5 years and the disease-free survival rate were 39.5% and 18.4%, respectively. The clinicopathologic features of the patients are summarized in Table 1.

We also investigated 39 patients with ICC and 59 patients with metastatic liver tumors from primary colorectal cancer who had undergone initial surgical resection between 1991 and 2005 at the National Cancer Center Hospital. The patients with ICC or metastatic liver cancer without hepatitis viral infection were randomly selected and those with hepatitis viral infection were all the patients we had. The patients with ICC comprised 22 males and 17 females, and their median age at surgery was 63 years (range, 44-85 years). HBV and HCV infection were detected in four and five patients, respectively. Their livers were diagnosed histopathologically as CH in eight patients and as PC in one patient. NCH were found in the liver of 30 patients without any HBV or HCV infection. Tumor diameters ranged from 15 to 140 mm (mean, 64.6 ± 30.6 mm). There were 8 patients at stage I, 9 patients at stage II, 3 patients at stage IIIa, 7 patients at stage IIIb, and 12 patients at stage IIIc according to the International Union against Cancer staging classification (31). ICCs were classified histopathologically as well-differentiated adenocarcinoma in 7 cases, moderately differentiated adenocarcinoma in 27, and poorly differentiated adenocarcinoma in 5 according to the WHO classification (30). The patients with liver metastasis from colorectal cancer comprised 37 males and 22 females, and their median age at surgery was 62 years (range, 34-81 years). HBV and HCV virus infection were detected in 8 and 21 patients, respectively, and their livers were diagnosed histopathologically as CH in 18 and as NCH in 11. The other 30 patients had not been infected with HBV or HCV and their nontumorous liver showed no inflammatory or fatty changes. Therefore, the nontumorous liver tissue from these patients was defined as "healthy liver." Thirty-three patients had a solitary tumor and 26 had multiple tumors. Tumor diameters ranged from 12 to 150 mm

Table 1. Clinicopathologic features of the patients

Variables	Results
Characteristics of the patients with HCC (218 cases)	
Age, y (median, range)	62, 17-84
Gender (male/female)	170/48
Virus infection [HBV/HCV/HBV+HCV/(-)]	57/117/10/34
Nontumor liver (NCH/CH/PC/LC)	20/101/35/62
Tumor nodules (AH/AAH/early HCC/WD HCC/MD HCC/PD HCC)	11/9/68/58/123/54
Clinicopathologic findings of the patients with HCC (147 cases)	
Age, y (median, range)	62, 17-83
Gender (male/female)	113/34
Virus infection [HBV/HCV/HBV+HCV/(-)]	47/79/9/12
Nontumor liver (NCH/CH/PC/LC)	17/71/23/36
Child-Pugh classification (A/B/C)	136/11/0
TNM stage (I/II/III/IV)	57/53/37/0
Histologic grade (early HCC/WD HCC/MD HCC/PD HCC)	17/15/77/38
AFP, ng/mL (median, range)	27.1, 1-27,170
VP (presence/absence)	57/90
IM (presence/absence)	33/114
Tumor size, mm (median, range)	35, 6-185

Abbreviations: MD, moderately differentiated; PD, poorly differentiated; WD, well differentiated.

(mean, 42.3 ± 28.2 mm). Histopathologically, the tumors were well-differentiated adenocarcinoma in 5 cases, moderately differentiated adenocarcinoma in 53 cases, and poorly differentiated adenocarcinoma in 1 case.

Immunohistochemical analysis. Immunohistochemistry was done on the formalin-fixed, paraffin-embedded tissue sections as described previously (33). We reacted 4- μ m-thick sections of representative blocks with monoclonal antibodies against the following: CD4 (1F6; 1:50), CD8 (4B11; 1:50), and perforin (5B11; 1:50) from Novocastra Laboratories, Ltd. (Newcastle upon Tyne, United Kingdom), and FOXP3 (clone 42; ref. 25). Briefly, the sections were deparaffinized and rehydrated. After blocking of endogenous peroxidase with methanol containing 0.3% H₂O₂, the sections were autoclaved at 121°C for 10 min in citrate buffer (10 mmol/L sodium citrate; pH 6.0) for antigen retrieval. After blocking with normal goat serum, the sections were reacted overnight with appropriately diluted primary antibodies. The sections were then reacted sequentially with biotin-conjugated anti-mouse IgG antibodies (Vector Laboratories, Burlingame, CA) and Vectastain Elite ABC reagent (Vector Laboratories). For staining CD4 and CD8, a CSA system (DAKO, Glöstrup, Denmark) and EnVision⁺ Polymer system (DAKO) were used, respectively, instead of the avidin-biotin complex system. Diaminobenzidine was used as the chromogen, and the nuclei were counterstained with hematoxylin.

Serial sections were prepared from each paraffin block. The first section was stained with H&E and the second, third, and fourth sections were subjected to immunohistochemistry to detect the CD8, CD4, and FOXP3 antigens. CD8⁺, CD4⁺, or FOXP3⁺ lymphocytes were counted in the corresponding visual fields. Quantitative evaluation of lymphocytes was done by analyzing at least three different high-power fields ($\times 40$ objective and $\times 10$ eyepiece). The proportion of FOXP3⁺ lymphocytes among CD4⁺ lymphocytes and that of CD8⁺ lymphocytes among total T cells, together with the sum of CD4⁺ and CD8⁺ lymphocytes, were calculated for each field and the averages were compared.

Statistical analysis. Values were expressed as mean \pm SD. Statistical analyses were done with StatView-J 5.0 software (Abacus Concepts, Berkeley, CA). Associations among the variables were assessed by the χ^2 test, Student's *t* test, Mann-Whitney *U* test, and Kruskal-Wallis test. If there was evidence of non-normality, the Mann-Whitney *U* test or the Kruskal-Wallis test was used to test the difference in medians among the groups. Survival rates were calculated by the Kaplan-Meier method. Differences between survival curves were analyzed by the log-rank test.

To assess the correlation between survival time and multiple clinicopathologic variables, multivariate analyses were done by the Cox proportional hazards regression model. Differences were considered significant at $P < 0.05$.

Results

Increased populations of FOXP3⁺ Tregs among CD4⁺ T cells in tumor stroma of HCC. In order to assess the infiltration of Tregs in the stroma of HCC ($n = 235$) and nontumorous liver ($n = 248$), we evaluated both the absolute numbers of FOXP3⁺ Tregs and the prevalence of FOXP3⁺ Tregs among CD4⁺ T cells. The absolute number of FOXP3⁺ Tregs that had infiltrated HCC was significantly higher than that of Tregs in nontumorous liver from patients with HCC or healthy liver tissue (versus healthy controls, $P < 0.001$; versus NCH, $P < 0.001$; versus CH, $P = 0.002$; versus PC, $P = 0.023$; versus LC, $P < 0.001$; Fig. 1A). The prevalence of tumor-infiltrating FOXP3⁺ Tregs among CD4⁺ T cells in HCC was also significantly higher (versus healthy controls, $P < 0.001$; versus NCH, $P < 0.001$; versus CH, $P < 0.001$; versus PC, $P < 0.001$; versus LC, $P < 0.001$; Fig. 1B). Among advanced HCCs, the prevalence of FOXP3⁺ Tregs was significantly higher in less differentiated HCCs (Kruskal-Wallis test, $P < 0.001$; Fig. 1B). No significant difference in the infiltration of Tregs was found among CH, PC, and LC. The prevalence of Tregs in NCH was lower than that in CH ($P = 0.021$), PC, and LC, but was significantly higher than that in healthy controls ($P < 0.001$; Fig. 1B).

The absolute number of CD8⁺ T cells was increased in CH, PC, and LC, and was significantly higher than that in HCC ($P < 0.001$; Fig. 1C). The prevalence of CD8⁺ T cells in HCC was significantly lower than that in any type of damaged and nontumorous liver from patients with HCC (versus NCH, $P = 0.025$; versus CH, $P < 0.001$; versus PC, $P = 0.015$; versus LC, $P < 0.001$; Fig. 1D). In advanced HCCs, the prevalence of CD8⁺ T cells was significantly lower in less differentiated HCC (Kruskal-Wallis test, $P = 0.034$; Fig. 1D). CD8⁺ T cells

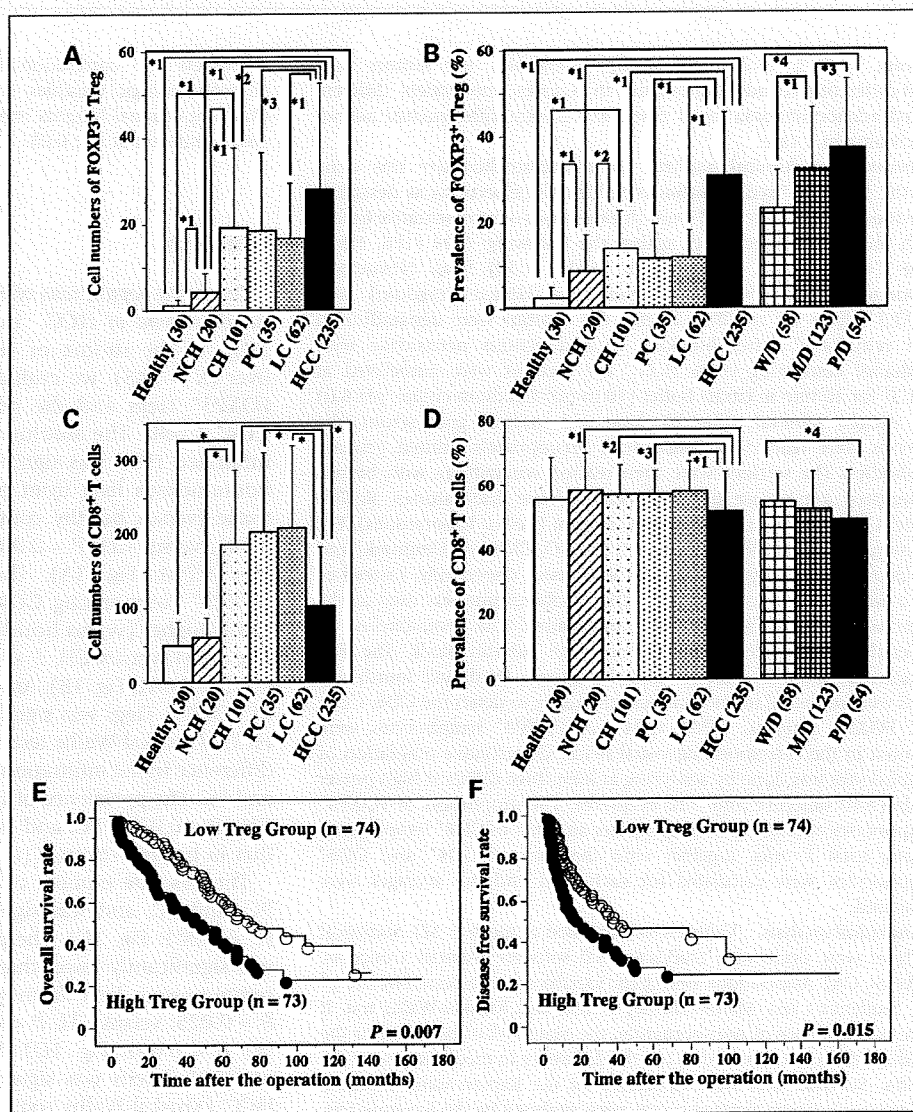
were increased slightly in NCH and viral hepatitis including CH, PC, and LC compared with healthy controls. These results suggested that an immunoreaction had also occurred in non-tumorous liver bearing HCC without viral hepatitis.

Clinicopathologic features of HCC and the prevalence of tumor-infiltrating Tregs and CD8⁺ T cells. We analyzed the correlation between clinicopathologic features of HCC and the prevalence of tumor-infiltrating Tregs or that of CD8⁺ T cells in HCC (Table 2A and B). Patients with HCC were divided into two groups either by the median value for the prevalence of tumor-infiltrating Tregs (29.0%) or by CD8⁺ T cells (51.5%). The high Treg group ($n = 73$) showed a significant correlation with high histologic grade ($P = 0.021$) and tended to show a lower number of infiltrating CD8⁺ T cells in HCC ($P = 0.064$) among the various clinicopathologic characteristics (Table 2A).

Prognostic significance of the prevalence of Tregs and CD8⁺ T cells in HCC. Overall and disease-free survival were analyzed in these patients. Of the 147 patients with HCC who underwent hepatic resection, 88 (59.9%) died. The overall 5-year survival

and disease-free survival rates were 39.5% and 18.4%, respectively. The low-Treg group showed significantly better overall survival than the high-Treg group (log-rank test, $P = 0.007$; Fig. 1E). Mean overall survival was 60.3 (± 33.8) months for the low-Treg group and 45.1 (± 38.7) months for the high-Treg group. The low-Treg group also showed significantly better disease-free survival than the high-Treg group (log-rank test, $P = 0.015$; Fig. 1F). Mean disease-free survival was 36.2 (± 31.7) months for the low-Treg group and 27.3 (± 32.9) months for the high-Treg group. The 15 clinicopathologic factors listed in Table 3A and B were examined for their association with overall and disease-free survival after initial resection of the tumor. Univariate analysis of overall survival revealed that the following variables had a negative influence: Child-Pugh classification (B), TNM stage (III and IV), high serum α -fetoprotein (AFP; >27.1 IU/mL), presence of portal vein invasion (VP), presence of histologic intrahepatic metastatic foci (IM), and high prevalence of tumor-infiltrating Tregs (Table 3A). In multivariate Cox proportional hazard analysis for clinicopathologic variables and prevalence of tumor-infiltrating Tregs, the

Fig. 1. Increased population of FOXP3⁺ Tregs and decreased population of CD8⁺ T cells in tumor stroma of HCC. **A** and **B**, absolute number of Tregs (**A**) and prevalence of Tregs (**B**) in HCC and nontumorous liver. Right column, the contents of HCC according to histologic grade (**B**). Number of cases tested in parentheses: **A**, *1, $P < 0.001$; *2, $P = 0.002$; *3, $P = 0.023$. **B**, *1, $P < 0.001$; *2, $P = 0.021$; *3, $P = 0.044$; *4, $P < 0.001$ (Kruskal-Wallis test); thin bars, SD. **C** and **D**, absolute number of CD8⁺ T cells (**C**) and prevalence of CD8⁺ T cells (**D**) in HCC and nontumorous liver. Right column, the contents of HCC according to histologic grade (**D**). Number of cases tested in parentheses: thin bars, SD. **C**, *1, $P < 0.001$. **D**, *1, $P = 0.025$; *2, $P < 0.001$; *3, $P = 0.015$; *4, $P < 0.001$ (Kruskal-Wallis test). **E** and **F**, Kaplan-Meier survival curves of 147 patients with HCC. Overall survival curve (**E**) and disease-free survival curve (**F**) are shown. The prognosis was significantly worse in the high Treg prevalence group (solid dots, $n = 73$) than in the low Treg prevalence group [white dots, $n = 74$; log-rank test, $P = 0.007$ (**E**) and $P = 0.015$ (**F**)].



hazard ratio for poor prognosis was 1.640 for patients in the high-Treg group compared with patients in the low-Treg group ($P = 0.040$; Table 3A). Worse Child-Pugh classification and the presence of VP were also independent factors for overall patient survival. Univariate analysis for disease-free survival revealed that six variables negatively affected the survival rate and all of them were the same with the six variables of overall survival (Table 3B). In multivariate analysis for disease-free survival, two variables—the presence of IM and the high prevalence of Tregs infiltrating HCC—were significant factors. The hazard ratio for poor prognosis was 1.706 for patients in the high-Treg group compared with patients in the low-Treg group ($P = 0.024$; Table 3B). There was no significant difference in the overall survival rate or disease-free survival rate between the low and high CD8⁺ T cell groups. These results indicated that the prevalence of tumor-infiltrating Tregs was an independent prognostic factor in patients with HCC, whereas the prevalence of tumor-infiltrating CD8⁺ T cells was not.

Increased populations of Tregs among CD4⁺ T cells in tumor stroma correspond to progression during multistage hepatocarcinogenesis. It was suggested that Tregs play important roles in the progression of HCC. Therefore, the prevalence of Tregs among CD4⁺ T cells in the precursor lesions, AH ($n = 11$; Fig. 2E-H) and AAH ($n = 9$), and early HCC ($n = 68$; Fig. 2I-L), was analyzed during tumorigenesis of HCC. As shown in Fig. 3A, the prevalence of Tregs increased significantly in a stepwise manner during the progression of hepatocarcinogenesis (Kruskal-Wallis test, $P < 0.001$; viral hepatitis containing CH, PC, and LC versus precursor lesions containing AH and AAH, $P = 0.038$; precursor lesions versus early HCC, $P = 0.121$; early HCC versus advanced HCC, $P < 0.001$). These findings suggest that the prevalence of Tregs is closely correlated with the progression of multistage hepatocarcinogenesis. In contrast, the prevalence of CD8⁺ T cells showed a clear, but not drastic, decrease during the progression of hepatocarcinogenesis (Kruskal-Wallis test, $P < 0.001$; Fig. 3B).

Table 2. Correlation between clinicopathologic findings and the prevalence of Tregs and CD8⁺ T cells infiltrating HCC

(A) Correlation between clinicopathologic findings and the prevalence of Tregs infiltrating HCC

Variables	Prevalence of Tregs among CD4 ⁺ T cells		
	High Treg	Low Treg	P
Age, y (mean ± SD)	62.6 ± 8.92	61.4 ± 10.4	0.444*
Gender (male/female)	59/14	54/20	0.259 [†]
Viral infection			
HBV and/or HCV/(–)	66/7	69/5	0.531 [†]
HBV(+)/(–)	27/7	29/5	0.525 [†]
HCV(+)/(–)	45/7	43/5	0.640 [†]
Nontumor liver (NCH/CH/PC/LC)	7/41/9/16	10/30/14/20	0.289 [†]
Child-Pugh score (A/B/C)	68/5/0	68/6/0	0.772 [†]
TNM stage (I/II/III/IV)	28/22/23/0	29/31/14/0	0.155 [†]
Tumor size, mm (median, range)	40, 9-185	30, 6-150	0.113 [†]
Histologic grade (early HCC/WD HCC/MD HCC/PD HCC)	7/3/38/25	10/12/39/13	0.021[†]
AFP, ng/mL (median, range)	24.1 (1.8-27,170)	28.3 (1.0-25,000)	0.681 [†]
VP (presence/absence)	33/40	24/50	0.112 [†]
IM (presence/absence)	20/53	13/61	0.152 [†]
Number of CD8 ⁺ T cells infiltrating tumor (median, range)	75 (12-405)	91 (9-435)	0.064 [†]

(B) Correlation between clinicopathologic findings and the prevalence of CD8⁺ T cells infiltrating HCC

Variables	Prevalence of CD8 ⁺ T cells in total T cells		
	High CD8 ⁺ T cells	Low CD8 ⁺ T cells	P
Age, y (mean ± SD)	63.6 ± 9.08	60.5 ± 10.0	0.051*
Gender (male/female)	51/23	62/12	0.045[†]
Viral infection			
HBV and/or HCV/(–)	69/4	66/8	0.238 [†]
HBV(+)/(–)	30/4	26/8	0.203 [†]
HCV(+)/(–)	42/4	46/8	0.348 [†]
Nontumor liver (NCH/CH/PC/LC)	11/35/12/15	6/36/11/21	0.471 [†]
Child-Pugh score (A/B/C)	67/6/0	69/5/0	0.736 [†]
TNM stage (I/II/III/IV)	28/29/16/0	29/24/21/0	0.560 [†]
Tumor size, mm (median, range)	40, 6-185	31, 10-150	0.075 [†]
Histologic grade (early HCC/WD HCC/MD HCC/PD HCC)	9/8/39/17	8/7/38/21	0.907 [†]
AFP, ng/mL (median, range)	21.5 (1.0-27,170)	36.3 (1.8-17,430)	0.105 [†]
VP (presence/absence)	31/42	26/48	0.362 [†]
IM (presence/absence)	18/55	15/59	0.524 [†]

Abbreviations: MD, moderately differentiated; PD, poorly differentiated; WD, well differentiated.

*Student's *t* test.

[†]χ² test or Fisher exact test.

[‡]Mann-Whitney *U* test.

Table 3. Univariate and multivariate analyses of prognosis factors associated with overall and disease-free survival in patients with HCC

Variables	Univariate analysis		Multivariate analysis	
	Hazard ratio (95% confidence interval)	P	Hazard ratio (95% confidence interval)	P
(A) Univariate and multivariate analyses of prognosis factors associated with overall survival in patients with HCC				
Prevalence of tumor-infiltrating FOXP3 ⁺ Tregs among CD4 ⁺ T cells in HCC (high/low)	1.791 (1.163-2.760)	0.008	1.640 (1.023-2.628)	0.040
Prevalence of tumor-infiltrating CD8 ⁺ T cells in total T cells in HCC (high/low)	1.055 (0.687-1.620)	0.806	1.109 (0.681-1.805)	0.678
Age* (>63 y/<63 y)	1.003 (0.653-1.540)	0.989	0.909 (0.573-1.440)	0.684
Gender (male/female)	1.052 (0.636-1.740)	0.844	0.957 (0.554-1.655)	0.876
Viral hepatitis (presence/absence)	1.140 (0.496-2.620)	0.757	0.972 (0.332-2.842)	0.958
Nontumor liver (NCH/CH, PC, LC)	0.766 (0.369-1.592)	0.475	0.503 (0.207-1.225)	0.130
Child-Pugh score (A/B, C)	0.462 (0.222-0.962)	0.039	0.395 (0.171-0.913)	0.030
TNM stage (I, II/III, IV)	0.412 (0.256-0.663)	<0.001	1.079 (0.456-2.548)	0.863
Tumor size* (>37 mm/<37 mm)	1.398 (0.909-2.149)	0.127	1.018 (0.553-1.875)	0.954
AFP* (>27.1 ng/mL/<27.1 ng/mL)	1.673 (1.084-2.581)	0.020	1.454 (0.901-2.347)	0.125
Histologic grade (WD HCC/MD HCC, PD HCC)	0.637 (0.376-1.078)	0.093	0.931 (0.489-1.772)	0.828
VP (presence/absence)	2.843 (1.825-4.429)	<0.001	2.546 (1.323-4.900)	0.005
IM (presence/absence)	2.880 (1.786-4.641)	<0.001	2.081 (0.916-4.730)	0.080
Prevalence CD8 ⁺ T cells in total T cells in nontumor liver (high/low)	0.754 (0.490-1.159)	0.198	0.688 (0.419-1.131)	0.140
Prevalence of FOXP3 ⁺ Tregs among CD4 ⁺ T cells in nontumor liver (high/low)	0.756 (0.491-1.165)	0.205	0.737 (0.442-1.229)	0.241
(B) Univariate and multivariate analyses of prognosis factors associated with disease-free survival in patients with HCC				
Prevalence of tumor-infiltrating FOXP3 ⁺ Tregs among CD4 ⁺ T cells in HCC (high/low)	1.701 (1.105-2.619)	0.016	1.706 (1.073-2.713)	0.024
Prevalence of tumor-infiltrating CD8 ⁺ T cells in total T cells in HCC (high/low)	1.150 (0.750-1.765)	0.522	1.330 (0.817-2.165)	0.251
Age* (>63 y/<63 y)	0.917 (0.597-1.407)	0.691	0.803 (0.508-1.271)	0.350
Gender (male/female)	0.992 (0.600-1.641)	0.976	0.941 (0.546-1.619)	0.825
Viral hepatitis (presence/absence)	0.931 (0.405-2.140)	0.866	0.754 (0.249-2.287)	0.619
Nontumor liver (NCH/CH, PC, LC)	0.902 (0.435-1.871)	0.782	0.537 (0.215-1.342)	0.184
Child-Pugh score (A/B, C)	0.458 (0.220-0.955)	0.037	0.463 (0.206-1.039)	0.062
TNM stage (I, II/III, IV)	0.357 (0.220-0.577)	<0.001	0.808 (0.320-2.038)	0.651
Tumor size* (>37 mm/<37 mm)	1.455 (0.947-2.235)	0.087	1.171 (0.635-2.159)	0.614
AFP* (>27.1 ng/mL/<27.1 ng/mL)	1.556 (1.010-2.397)	0.045	1.503 (0.932-2.421)	0.944
Histologic grade (WD HCC/MD HCC, PD HCC)	0.810 (0.481-1.365)	0.429	1.354 (0.722-2.538)	0.345
VP (presence/absence)	2.284 (1.476-3.535)	<0.001	1.692 (0.870-3.294)	0.121
IM (presence/absence)	3.512 (2.163-5.704)	<0.001	2.487 (1.020-6.064)	0.045
Prevalence CD8 ⁺ T cells in total T cells in nontumor liver (high/low)	0.727 (0.473-1.118)	0.146	0.644 (0.393-1.054)	0.080
Prevalence of FOXP3 ⁺ Tregs among CD4 ⁺ T cells in nontumor liver (high/low)	0.800 (0.520-1.230)	0.309	0.788 (0.482-1.290)	0.344

Abbreviations: MD, moderately differentiated; PD, poorly differentiated; WD, well differentiated.

*Two groups were divided by the median.

Infiltration of Tregs shows no difference among different histologic types of tumor, but differs between primary and metastatic hepatic tumors. Although metastatic liver tumors are common, the most frequent type of tumor developing primarily in the liver is HCC, and the second major type is ICC. In order to examine whether antitumor immune response was affected by tumor histology, we compared the prevalence of Tregs and CD8⁺ T cells between HCC and primary hepatic adenocarcinoma, ICC ($n = 39$). The prevalence of Tregs in the tumor stroma was comparable between HCC and ICC (Fig. 4A), whereas the prevalence of CD8⁺ T cells in ICC was significantly lower than that in HCC ($P = 0.004$; Fig. 4A). The prevalence of Tregs in nontumorous liver was also comparable between patients with HCC and patients with ICC (Fig. 4B),

although their prevalence was significantly higher than that in healthy liver (versus HCC, $P < 0.001$; versus ICC, $P < 0.001$). The prevalence of CD8⁺ T cells in nontumorous liver was comparable among patients with HCC, ICC, and healthy liver. These findings suggest that the Treg response is almost the same in both histologic types of primary hepatic tumor, HCC, and ICC, whereas the CD8⁺ T cell response is reduced to a greater degree in ICC than in HCC.

We then analyzed the prevalence of tumor-infiltrating Tregs and CD8⁺ T cells in the liver of patients with primary HCC, its IM ($n = 27$), ICC ($n = 39$), and metastatic liver adenocarcinoma originating from colorectal cancer ($n = 59$), to examine whether the antitumor immune response differs between primary and metastatic tumors of the liver. The prevalence of Tregs



Fig. 2. Representative features of tissue-infiltrating FOXP3⁺, CD4⁺, or CD8⁺ T lymphocytes. CH (A-D), AH (E-H), early HCC (I-L), and MD HCC (M-P) by HE staining (A, E, I, and M) and immunostaining for FOXP3 (B, F, J, and N), CD4 (C, G, K, and O), and CD8 (D, H, L, and P).

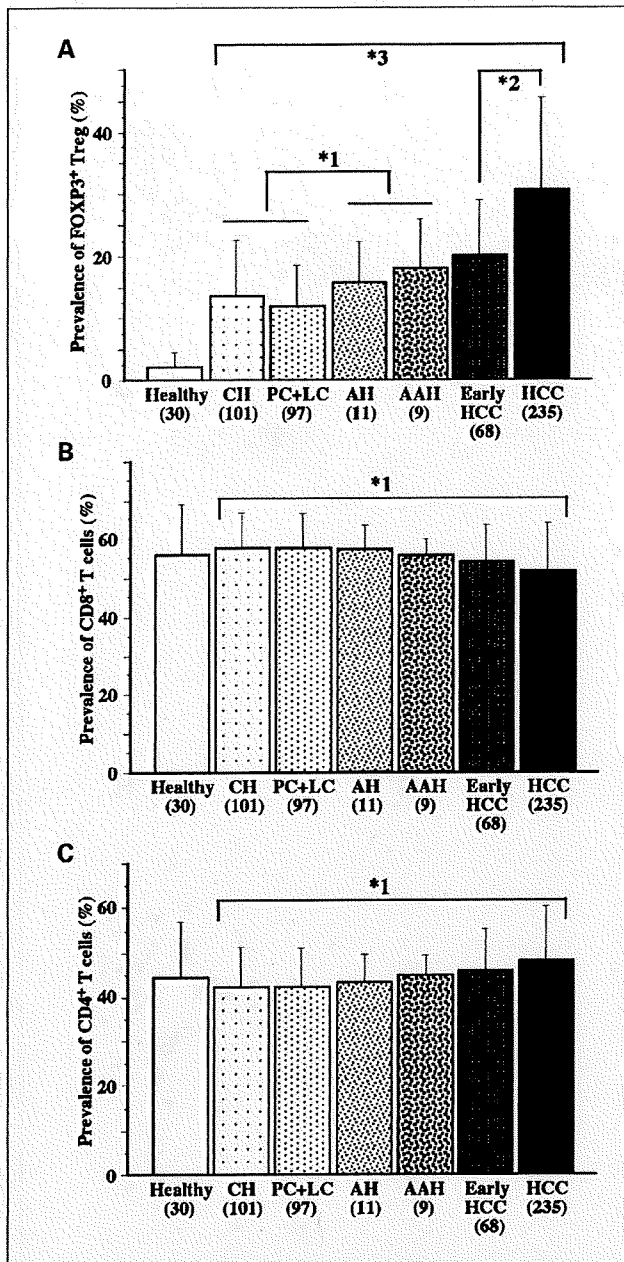


Fig. 3. Increased population of Tregs and decreased population of CD8⁺ T cells in tumor stroma corresponding to the progression of multistage hepatocarcinogenesis. Prevalence of Tregs among CD4⁺ T cells (A), prevalence of CD8⁺ T cells among total T cells (B), and prevalence of CD4⁺ T cells among total T cells (C) in HCC, its precursor lesions, and nontumorous liver. Number of cases tested in parentheses; Thin bars, SD. A, *1, $P = 0.038$; *2, $P < 0.001$; *3, $P < 0.001$ (Kruskal-Wallis test). B and C, *1, $P < 0.001$ (Kruskal-Wallis test).

was significantly higher in primary HCC than in IM ($P = 0.003$; Fig. 4A). Also, the prevalence of Tregs in primary hepatic adenocarcinoma was higher than that in metastatic hepatic adenocarcinoma ($P = 0.020$; Fig. 4A). The prevalence of CD8⁺ T cells was comparable between primary and metastatic tumors.

Hepatitis viral infection and antitumor host immune response. HBV or HCV infection is a risk factor for the development of HCC (2), and it is also reported that these chronic viral infections suppress the host immune response (2).

Some investigators have suggested that HCV infection increases ICC development, although this remains to be proven (34). The prevalence of Tregs in nontumorous liver of patients infected with HBV or HCV was significantly higher than in healthy liver (Fig. 4B), even in patients who were in the so-called "carrier" stage, with infection but no detectable manifestations or histologic changes. To investigate whether Tregs affected the development of primary liver tumors, we compared the prevalence of Tregs in nontumorous areas of liver bearing HCC, ICC, or metastatic liver adenocarcinoma among patients with and without hepatitis viral infection. The prevalence of Tregs in nontumorous liver bearing HCC or ICC without any HBV or HCV infection was apparently higher than that in healthy liver (versus HCC, $P < 0.001$; versus ICC, $P < 0.001$; Fig. 4B). In contrast, the prevalence of Tregs in nontumorous liver bearing HCC or ICC with HBV or HCV infection was slightly, but not significantly, higher than that in liver bearing no primary liver tumor with hepatitis virus infection (Fig. 4B). These findings suggest that a further increase of Treg infiltration in nontumorous liver with hepatitis virus infection is not closely correlated with the development of primary liver tumors. An interesting observation was that the prevalence of Tregs in nontumorous liver bearing HCC without HBV or HCV infection was higher than that in HBV-infected liver (Fig. 4B and C). The prevalence of Tregs in liver infected with HCV was higher than that in liver with HBV infection ($P = 0.016$), and

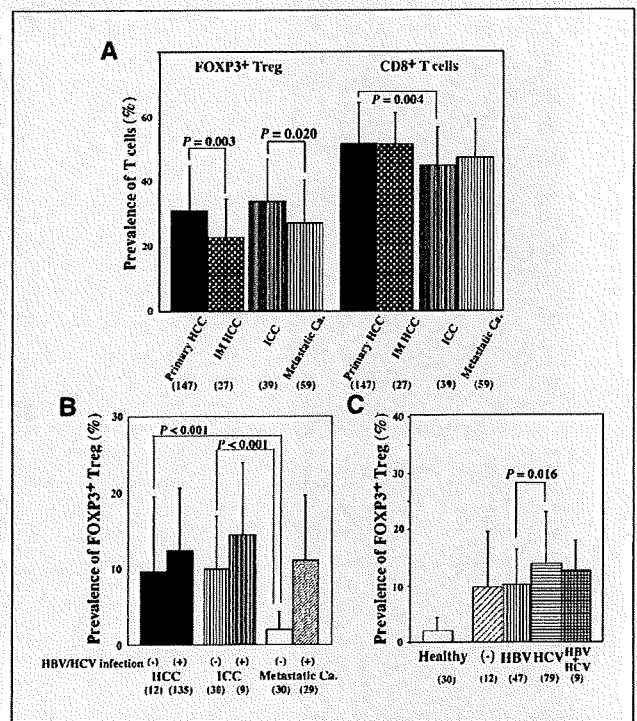


Fig. 4. A, prevalence of T cells in primary liver cancer (HCC and ICC) and metastatic HCC (IM) and adenocarcinoma from colon cancer (metastatic ca). Left and right columns, the prevalence of Tregs and CD8⁺ T cells, respectively. Number of cases tested are in parentheses. B, prevalence of Tregs in nontumorous liver of patients bearing HCC, ICC, or metastatic liver cancer, with or without HBV or HCV infection. Number of cases tested in parentheses. C, prevalence of Tregs in nontumorous liver of patients bearing HCC. Prevalence of Tregs in nontumorous liver with or without (-) hepatitis B and/or C viral infection were significantly higher than that in healthy controls. Number of cases tested in parentheses.

that in both HBV- and HCV-infected liver was intermediate between that in HBV- and HCV-infected liver. These observations were also recognized in patients with ICC (data not shown).

Discussion

Tumor-infiltrating lymphocytes represent the host immune response to a tumor, and include CD8⁺ cytotoxic T cells and natural killer cells as positive responders and Tregs as immunosuppressors. There has been no large-scale or clinicopathologic study of Tregs in HCC and tumor-infiltrating lymphocytes in hepatocarcinogenesis. In the present study, we investigated the relationship between host immune response and hepatocarcinogenesis, focusing especially on Treg infiltration. First, we showed the clinicopathologic significance of Tregs among CD4⁺ T cells infiltrating advanced HCC based on the following findings: (a) the prevalence of Tregs in HCC ($n = 235$) was significantly higher ($P < 0.001$) than that in nontumorous liver ($n = 248$), which included healthy liver, NCH, CH, PC, and LC. (b) Patients with HCC in the high-Treg group showed a significantly lower survival ratio. Both overall survival (log-rank test, $P = 0.007$) and disease-free survival (log-rank test, $P = 0.015$) were lower than for patients with HCC belonging to the low-Treg group. (c) Multivariate analysis revealed that the prevalence of tumor-infiltrating Tregs was an independent prognostic factor, along with Child-Pugh classification and presence of VP, for overall survival and that the prevalence of tumor-infiltrating Tregs and that of IM were independent prognostic factors for disease-free survival. (d) The prevalence of tumor-infiltrating Tregs was increased in poorly differentiated HCC (Kruskal-Wallis test; $P < 0.001$). In addition, we found that the prevalence of tumor-infiltrating Tregs increased in a stepwise manner (Kruskal-Wallis test, $P < 0.001$), whereas the prevalence of CD8⁺ T cells decreased (Kruskal-Wallis test, $P < 0.001$) during the progression of hepatocarcinogenesis. These findings suggest that Treg infiltration was closely correlated with the progression of neoplastic cells in hepatocarcinogenesis. Furthermore, we showed that the prevalence of Tregs was increased in nontumorous liver tissue from patients with primary hepatic tumors, regardless of the presence of hepatitis virus infection or histopathologically evident hepatitis or liver cirrhosis. This indicates that primary hepatic tumors develop in liver, in which Tregs show marked infiltration and immune reactivity is suppressed. This is the first report to show that infiltration of Tregs is closely correlated with the development and progression of hepatocarcinogenesis, and that the prevalence of Tregs is a useful prognostic factor in patients with HCC.

It was reported previously that CD8⁺ T cells infiltrating tumors are associated with good prognosis (8, 9), and that tumor-infiltrating Treg is increased in a variety of tumors (21–28). A few studies have also investigated the clinicopathologic significance of Treg infiltration (23–25), but conclusions about its correlation with prognosis were contradictory. Marked infiltration of Tregs in cancer stroma was reported to be an unfavorable prognostic factor in ovarian (23) and pancreatic (25) cancers, and was associated with control of tumor progression in head and neck cancers (24). No prognostic influence of Tregs was found in anal squamous cell carcinomas (35). In the present study, using multivariate analyses, we

showed that the prevalence of Tregs in HCC was significantly correlated with both overall survival and disease-free survival. A high prevalence of Tregs was closely correlated only with histologic grade among a number of clinicopathologic variables. These findings indicate that the prevalence of tumor-infiltrating FOXP3⁺ Tregs can be an independent prognostic factor for patients with HCC. In addition to the prevalence of Tregs, our multivariate analysis revealed that among 15 prognostic factors, Child-Pugh classification and the presence of VP and IM were independent indicators of unfavorable overall and disease-free survival, respectively, consistent with previous studies (36, 37). In contrast, infiltration of CD8⁺ T cells as well as perforin-positive cells (data not shown) in HCC was found to have no prognostic significance. A positive prognostic effect of infiltrating CD8⁺ T cells has been reported in various solid cancers such as colorectal (8) and ovarian (9) cancer. Only patients bearing HCC with exceptionally marked infiltration of CD8⁺ T cells were reported to have a good prognosis (10). It is interesting that a negative prognostic effect of CD8⁺ T cell infiltration has been observed in virus-related tumors, including EB virus-associated nasopharyngeal carcinomas (38) and human papilloma virus-associated anal carcinomas (35). This effect observed in other tumors was not observed in HCC, even though HCC is closely associated with hepatitis virus infection, and might be attributable to an organ-specific immune response.

In established HCC, Treg infiltration might play an important role in tumor progression and clinical behavior by modifying the host immune response. Furthermore, our data showed that the prevalence of Tregs increased in a stepwise manner from viral hepatitis containing CH, PC, and LC, to precursor lesions of AH and AAH, early HCC, and advanced HCC, indicating that Treg infiltration was closely involved in the progression of hepatocarcinogenesis ($P < 0.001$; Fig. 3A). It has been suggested that Tregs suppress the immune response through cell contact-dependent (12–14) or cell contact-independent mechanisms (15, 16), and that immune suppression occurs in several steps (12, 14, 16). Various immune cells could be the targets of Treg suppression, such as CD8⁺ T cells, CD4⁺CD25⁻ T cells, B cells, natural killer cells, natural killer T-cells, and dendritic cells (12, 14, 16, 39, 40). In this study, the prevalence of CD8⁺ tumor-infiltrating lymphocytes was found to decrease significantly during hepatocarcinogenesis ($P < 0.001$; Fig. 3B), and this was inversely correlated with Treg infiltration. The group of patients with advanced HCC showing marked Treg infiltration showed a tendency to have a lower prevalence of CD8⁺ tumor-infiltrating lymphocytes (Table 2A). Thus, it is possible that Tregs contribute to reducing the infiltration of CD8⁺ T cells during hepatocarcinogenesis. Unitt et al. reported that Tregs isolated from advanced HCC suppressed the proliferation and perforin expression of autologous circulating CD8⁺ T cells (27).

Persistent viral infection requires host immune suppression. CD4⁺CD25⁺ Tregs have been reported to be linked to the chronicity and progression of viral hepatitis in patients with HBV or HCV infection by down-regulating the hepatitis virus-specific T cell response (41–43). Our present observations confirm marked infiltration of Tregs in the liver of patients infected with HBV or HCV. Regardless of the presence of hepatitis virus infection and histopathologic changes indicative of hepatitis, the prevalence of Tregs in nontumorous liver tissue

of patients bearing HCC was significantly higher than that in healthy liver, but was slightly lower than that in liver with viral hepatitis. It has been suggested that even in patients with HCC of unknown etiology, immunosuppression might have started in the liver before tumor development. In patients with primary hepatic adenocarcinoma, ICC, the prevalence of FOXP3⁺ Tregs in nontumorous liver without viral infection was also higher than that in healthy liver. These findings suggest that primary hepatic tumors can develop in the liver with a certain degree of Treg infiltration. A subsequent increase of Treg infiltration seemed to accelerate the development of hepatic tumors in patients infected with hepatitis virus, but not to a significant degree. Further studies will be necessary to clarify the threshold of Treg prevalence at which the risk of hepatic tumor development becomes high. The prevalence of Tregs in primary hepatic tumors, both HCC and adenocarcinoma, was signifi-

cantly higher than that in metastatic hepatic tumors with the corresponding histology. These findings support the hypothesis that the development and progression of primary hepatic tumors involves high accumulation of Tregs.

In conclusion, our data suggest that Tregs play a role in controlling the immune response to HCC from the precursor stage to established cancer, and also that primary hepatic cancers might develop in liver that is immunosuppressed by marked infiltration of Tregs, regardless of the presence of hepatitis viral infection. A high prevalence of Tregs seems to be an indicator of poor prognosis.

Acknowledgments

The authors thank Rie Itoh, Yuko Yamauchi, and Kaoru Onozato for technical assistance.

References

- Llovet JM, Burroughs A, Bruix J. Hepatocellular carcinoma. *Lancet* 2003;362:1907–17.
- Kao JH, Chen DS. Overview of hepatitis B and C viruses. Infectious causes of Cancer. In: Goedert JJ, editor. New Jersey: Humana Press; 2000.
- Ueno Y, Moriyama M, Uchida T, Arakawa Y. Irregular regeneration of hepatocytes is an important factor in the hepatocarcinogenesis of liver disease. *Hepatology* 2001;33:357–62.
- Tsuda H, Hirohashi S, Shimosato Y, Terada M, Hasegawa H. Clonal origin of atypical adenomatous hyperplasia of the liver and clonal identity with hepatocellular carcinoma. *Gastroenterology* 1988;95:1664–6.
- Sakamoto M, Hirohashi S, Shimosato Y. Early stages of multistep hepatocarcinogenesis: adenomatous hyperplasia and early hepatocellular carcinoma. *Hum Pathol* 1991;22:172–8.
- Saito Y, Kanai Y, Sakamoto M, Saito H, Ishii H, Hirohashi S. Expression of mRNA for DNA methyltransferases and methyl-CpG-binding proteins and DNA methylation status on CpG islands and pericentromeric satellite regions during human hepatocarcinogenesis. *Hepatology* 2001;33:561–8.
- Chuma M, Sakamoto M, Yamazaki K, et al. Expression profiling in multistage hepatocarcinogenesis: identification of HSP70 as a molecular marker of early hepatocellular carcinoma. *Hepatology* 2003;37:198–207.
- Zhang L, Conejo-Garcia JR, Katsaros D, et al. Intratumoral T cells, recurrence, and survival in epithelial ovarian cancer. *N Engl J Med* 2003;348:203–13.
- Naito Y, Saito K, Shiiba K, et al. CD8⁺ T cells infiltrated within cancer cell nests as a prognostic factor in human colorectal cancer. *Cancer Res* 1998;58:3491–4.
- Wada Y, Nakashima O, Kutami R, Yamamoto O, Kojiro M. Clinicopathological study on hepatocellular carcinoma with lymphocytic infiltration. *Hepatology* 1998;27:407–14.
- Nakamoto Y, Suda T, Momoi T, Kaneko S. Different procarcinogenic potentials of lymphocyte subsets in a transgenic mouse model of chronic hepatitis B. *Cancer Res* 2004;64:3326–33.
- Sakaguchi S. Regulatory T cells: key controllers of immunologic self-tolerance. *Cell* 2000;101:455–8.
- Dieckmann D, Plottner H, Berchtold S, Berger T, Schuler G. *Ex vivo* isolation and characterization of CD4⁺CD25⁺ T cells with regulatory properties from human blood. *J Exp Med* 2001;193:1303–10.
- Shevach EM. CD4⁺CD25⁺ suppressor T cells: more questions than answers. *Nat Rev Immunol* 2002;2:389–400.
- Chen ML, Pittet MJ, Gorelik L, et al. Regulatory T cells suppress tumor-specific CD8 T cell cytotoxicity through TGF- β signals *in vivo*. *Proc Natl Acad Sci U S A* 2005;102:419–24.
- von Boehmer H. Mechanisms of suppression by suppressor T cells. *Nat Immunol* 2005;6:338–44.
- Fontenot JD, Rudensky AY. A well adapted regulatory contrivance: regulatory T cell development and the forkhead family transcription factor Foxp3. *Nat Immunol* 2005;6:331–7.
- Shimizu JS, Yamazaki S, Sakaguchi S. Induction of tumor immunity by removing CD25⁺CD4⁺ T cells: a common basis between tumor immunity and autoimmunity. *J Immunol* 1999;163:5211–8.
- Onizuka SI, Tawara J, Shimizu J, Sakaguchi S, Fujita T, Nakayama E. Tumor rejection by *in vivo* administration of anti-CD25 (interleukin-2 receptor α) monoclonal antibody. *Cancer Res* 1999;59:3128–33.
- Nishikawa H, Kato T, Tawara I, et al. Accelerated chemically induced tumor development mediated by CD4⁺CD25⁺ regulatory T cells in wild-type hosts. *Proc Natl Acad Sci U S A* 2005;102:9253–7.
- Woo EY, Chu CS, Goletz TJ, et al. Regulatory CD4⁺CD25⁺ T cells in tumors from patients with early-stage non-small lung cancer and late-stage ovarian cancer. *Cancer Res* 2001;61:4766–72.
- Liyanage UK, Moore TT, Joo HG, et al. Prevalence of regulatory T cells is increased in peripheral blood and tumor microenvironment of patients with pancreas or breast adenocarcinoma. *J Immunol* 2002;169:2756–61.
- Curiel TJ, Coukos G, Zou L, et al. Specific recruitment of regulatory T cells in ovarian carcinoma fosters immune privilege and predicts reduced survival. *Nat Med* 2004;10:942–9.
- Badoual C, Hans S, Rodriguez J, et al. Prognostic value of tumor-infiltrating CD4⁺ T-cell subpopulations in head and neck cancers. *Clin Cancer Res* 2006;12:465–72.
- Hiraoka N, Onozato K, Kosuge T, Hirohashi S. Prevalence of FOXP3⁺ regulatory T cells increases during the progression of pancreatic ductal adenocarcinoma and its premalignant lesions. *Clin Cancer Res* 2006;12:5423–34.
- Ormandy LA, Hillebrand T, Wedemeyer H, Manns MP, Greten TF, Korangy F. Increased populations of regulatory T cells in peripheral blood of patients with hepatocellular carcinoma. *Cancer Res* 2005;65:2457–64.
- Unitt E, Rushbrook SM, Marshall A, et al. Compromised lymphocytes infiltrate hepatocellular carcinoma: the role of T-regulatory cells. *Hepatology* 2005;41:722–30.
- Yang XH, Yamagiwa S, Ichida T, et al. Increase of CD4⁺CD25⁺ regulatory T cells in the liver of patients with hepatocellular carcinoma. *J Hepatol* 2006;45:254–62.
- Ruprecht CR, Gattorno M, Ferlito F, et al. Coexpression of CD25 and CD27 identifies Foxp3⁺ regulatory T cells in inflamed synovia. *J Exp Med* 2005;201:1793–803.
- Hirohashi S, Ishak KG, Kojiro M, et al. Hepatocellular carcinoma. In: Hamilton SR, Aaltonen LA, editors. Pathology and genetics of tumors of the digestive system. Lyon: IARC Press; 2000. p. 159–72.
- Greene FL, Page DL, Fleming ID, et al. AJCC cancer staging manual. 6th ed. Chicago: Springer; 2002. p. 131–44.
- Ishak K, Baptista A, Bianchi L, et al. Histological grading and staging of chronic hepatitis. *J Hepatol* 1995;22:696–9.
- Takahashi Y, Akishima-fukusawa Y, Kobayashi N, et al. Prognostic value of tumor architecture, tumor-associated vascular characteristics, and expression of angiogenic molecules in pancreatic endocrine tumors. *Clin Cancer Res* 2007;13:187–96.
- Okuda K, Nakanuma Y, Miyazaki M. Cholangiocarcinoma: recent progress. Part 1: Epidemiology and etiology. *J Gastroenterol Hepatol* 2002;17:1049–55.
- Grabenbauer GG, Lahmer G, Distel L, Niedobitek G. Tumor-infiltrating cytotoxic T cells but not regulatory T cells predict outcome in anal squamous cell carcinoma. *Clin Cancer Res* 2006;12:3355–60.
- Franco D, Capussotti L, Smadja C, et al. Resection of hepatocellular carcinomas: results in 72 European patients with cirrhosis. *Gastroenterology* 1990;98:733–8.
- Izumi R, Shimizu K, Ii T, et al. Prognostic factors of hepatocellular carcinoma in patients undergoing hepatic resection. *Gastroenterology* 1994;106:720–7.
- Oudejans JJ, Harijandi H, Kummer JA, et al. High numbers of granzyme B/CD8-positive tumor-infiltrating lymphocytes in nasopharyngeal carcinoma biopsies predict rapid fatal outcome in patients treated with curative intent. *J Pathol* 2002;198:468–75.
- Ghiringhelli F, Menard C, Terme M, et al. CD4⁺CD25⁺ regulatory T cells inhibit natural killer cell functions in a transforming growth factor- β -dependent manner. *J Exp Med* 2005;202:1075–85.
- Tadokoro CE, Shakhfar G, Shen S, et al. Regulatory T cells inhibit stable contacts between CD4⁺ T cells and dendritic cells *in vivo*. *J Exp Med* 2006;203:505–11.
- Cabrera R, Tu Z, Xu R, et al. An immunomodulatory role for CD4⁺CD25⁺ regulatory T lymphocytes in hepatitis C virus infection. *Hepatology* 2004;40:1062–73.
- Stoop JN, van der Molen RG, Baan CC, et al. Regulatory T cells contribute to the impaired immune response in patients with chronic hepatitis B virus infection. *Hepatology* 2005;41:771–8.
- Xu D, Fu J, Jin L, et al. Circulating and liver resident CD4⁺CD25⁺ regulatory T cells actively influence the antiviral immune response and disease progression in patients with hepatitis B. *J Immunol* 2006;177:739–47.

Prognostic Value of Tumor Architecture, Tumor-Associated Vascular Characteristics, and Expression of Angiogenic Molecules in Pancreatic Endocrine Tumors

Yu Takahashi,^{1,3} Yuri Akishima-Fukasawa,¹ Noritoshi Kobayashi,¹ Tsuyoshi Sano,² Tomoo Kosuge,² Yuji Nimura,³ Yae Kanai,¹ and Nobuyoshi Hiraoka¹

Abstract **Purpose:** It is difficult to predict the biological behavior of pancreatic endocrine tumors (PETs). Our aim was to evaluate the prognostic significance of certain variables in PETs. **Experimental Design:** The following variables were examined in 37 patients with PETs and then compared with other clinicopathologic characteristics: histologic tumor structure; microvessel density (MVD) measured by three different methods, including a unique method involving calculation of solid area MVD; endothelial proliferation; and the immunohistochemical expression of vascular endothelial growth factor-A and CXC chemokine CXCL-12. Intratumoral vascular structures were analyzed by double immunofluorescence using 30- μ m-thick sections. **Results:** The presence of focal and intensive solid growth of tumor cells (large solid nests; $P = 0.003$), low solid area MVD ($P = 0.002$), a high endothelial cell proliferation index (EPI; $P = 0.005$), and high expression of CXCL-12 in PET cells ($P = 0.018$) were significant unfavorable prognostic indicators. The predominant structure of the overall tumor histology and the expression of vascular endothelial growth factor-A did not separate aggressive PETs. In areas of focal solid growth, tumor-associated blood vessels had obviously low MVD and high EPI, and their structures were poorly formed with highly abnormal features, in comparison with other areas. High expression of CXCL-12 in tumor cells was significantly associated with variables representing tumor growth, hematogenous tumor spread, low MVD, high EPI, and the presence of large solid nests. **Conclusions:** This study has provided novel findings on the prognostic features of tumor architecture and tumor-associated angiogenesis in PETs. CXCL-12 is the first candidate molecule in association with neoangiogenesis in PETs.

Pancreatic endocrine tumors (PETs) are uncommon neoplasms, and their prognostication is difficult when based purely on the histologic architecture and cytologic features of the tumor. Only the presence of distant metastases and local invasion to surrounding organs is the definitive criterion of malignancy (1–3). During the last few decades, various prognostic variables representing the proliferative or invasive

ability of tumor cells have been reported, such as tumor size, mitotic rate, Ki-67 proliferative index, and presence of vascular and perineural invasion (1–5). Other molecules have also been reported to be prognostic variables, such as cytokeratin 19 and CD99 (6, 7). The last WHO classification of PETs used some of these variables, in addition to conventional histopathologic tumor typing (1). However, this is still not enough for predicting the biological behavior of PETs because retrospective studies have shown that patients with PETs classified as “well-differentiated endocrine tumors,” “benign tumors,” or “tumors of uncertain behavior” sometimes suffer tumor recurrence or die of the disease (4, 6). To identify more reliable prognostic variables representing the biological characteristics of PETs, we analyzed their histologic structure, focusing especially on the solidness of the tumor growth pattern and attempted to classify them on this basis. At the same time, we examined the characteristics of intratumoral (i.t.) blood vessels, as these are closely associated with tumor architecture. In our experience, microvessel density (MVD) is lower in areas where tumor cells of PETs grow in a more solid pattern.

Normal endocrine tissues, including pancreatic islets of Langerhans and endocrine tumors, are characterized by high vascular density. In a murine pancreatic endocrine carcinoma model, RIP1-Tag2 transgenic mice expressing the SV40 T antigen in insulin-producing β cells, the tumor vasculature increases, and

Authors' Affiliations: ¹Pathology Division, National Cancer Center Research Institute; ²Division of Hepatobiliary and Pancreatic Surgery, National Cancer Center Hospital, Tokyo, Japan; and ³Division of Surgical Oncology, Department of Surgery, Nagoya University Graduate School of Medicine, Nagoya, Japan

Received 6/12/06; revised 10/5/06; accepted 10/18/06.

Grant support: Ministry of Health, Labor, and Welfare of Japan grant-in-aid for Third-Term Comprehensive 10-Year Strategy for Cancer Control and Ministry of Education, Culture, Sports, Science, and Technology of Japan grant-in-aid for Scientific Research.

The costs of publication of this article were defrayed in part by the payment of page charges. This article must therefore be hereby marked *advertisement* in accordance with 18 U.S.C. Section 1734 solely to indicate this fact.

Note: Supplementary data for this article are available at Clinical Cancer Research Online (<http://clincancerres.aacrjournals.org/>).

Requests for reprints: Nobuyoshi Hiraoka, Pathology Division, National Cancer Center Research Institute, 5-1-1 Tsukiji, Chuo-ku, Tokyo 104-0045, Japan. Phone: 81-3-3542-2511; Fax: 81-3-3248-2463; E-mail: nhiraoka@gan2.res.ncc.go.jp.

©2007 American Association for Cancer Research.

doi:10.1158/1078-0432.CCR-06-1408

vascular morphology become abnormal during multistep carcinogenesis (8, 9). Tumor-associated blood vessels in various human cancers are structurally and functionally abnormal, showing increased permeability, delayed maturation, and potential for rapid proliferation (10, 11). The vessel defects may also facilitate hematogenous spread of tumor cells (12). Angiogenesis is essential for tumor growth and also plays an important role in hematogenous spread (13, 14). Measurement of MVD using immunohistochemistry is a widely used method for measuring angiogenic activity. Numerous studies have shown that elevated MVD is a significant predictive indicator of poor survival (13, 15). In human PETs, however, some recent studies have shown that low MVD is an unfavorable prognostic factor (16, 17), whereas others have suggested that MVD is not a predictive indicator of survival (18, 19). Thus, the relationship between MVD and biological behavior in human PETs is still controversial, although high MVD does not seem to be an unfavorable prognostic factor. It has been shown that angiogenic factors in many kinds of human cancers are related to metastatic dissemination, tumor aggressiveness, and short patient survival (20–22). Only vascular endothelial growth factor-A (VEGF-A) has been studied in human PETs, although there is still no evidence that it contributes to malignancy or patient survival (16–18). No attempt has been made to assess the prognostic value of angiogenic factors other than VEGF-A in PETs.

The aim of the present study was to investigate histologic tumor architecture, tumor-associated angiogenesis, and expression of angiogenic molecules in a series of resected PETs and to evaluate the potential prognostic significance of these variables.

Materials and Methods

Patients and samples. This study was approved by the Ethics Committee of the National Cancer Center, Tokyo, Japan. Clinical and pathologic data and the specimens used for immunohistochemical analysis were obtained through a detailed retrospective review of the medical records of all 37 Japanese patients with PETs who had undergone initial surgical resection between 1981 and 2004 at the National Cancer Center Central Hospital, Japan. The median age of the patients at surgery was 55 years (range, 18–81 years; mean, 52.9 years). None of the patients

had received prior therapy and underwent potentially curative resection: pancreatoduodenectomy in 19 cases, distal pancreatectomy in 12 cases, tumor enucleation in 4 cases, and total pancreatectomy in 2 cases. Tumors were classified according to the WHO classification (1) into the following groups: benign well-differentiated endocrine tumors (referred to as WHO-1 in this report), well-differentiated endocrine tumors of uncertain behavior (WHO-2), well-differentiated endocrine carcinoma (WHO-3), and poorly differentiated endocrine carcinoma (WHO-4). Follow-up was available in all cases and ranged from 2 to 275 months (median, 46.8 months; mean, 65.2 months). During the follow-up period, nine patients presented with evidence of disease progression as liver metastasis, and two of them presented with evidence of local recurrence. The latest survival data were collected on December 31, 2004. The total survival rate was 78% at 5 years and 65% at 10 years. The clinicopathologic features of the patients are summarized in Table 1. Eight variables (large tumor size, presence of invasion to surrounding organs, presence of lymph node metastasis, presence of hematogenous metastasis, presence of vascular invasion, presence of perineural invasion, absence of functional hormone syndrome, and high Ki-67 index) had been reported to be unfavorable prognostic factors (1, 2). In our series, all these variables except "absence of functional hormone syndrome" were closely correlated with short survival (Table S1).

For histopathologic examinations, all tissue specimen was cut to make sections. Four-micrometer formalin-fixed, paraffin-embedded sections were prepared and stained with H&E. Vascular invasion was assessed by histopathologic examination, using H&E-stained tissue sections and sections stained for elastic fibers with Maeda's resorcin/fuchsin solution (Muto Pure Chemicals, Tokyo, Japan). With regard to the structural pattern of tumor histology, tumors were divided into four groups by the following criteria based on predominant architecture (Fig. 1A-D): grade 1, tumors consisting of small nests (with 1-5 tumor cells in the minor axis); grade 2, tumors consisting of moderate nests (with 6-10 tumor cells in the minor axis); grade 3, tumors consisting of large solid nests (with ≥11 tumor cells in the minor axis); and grade 4, tumors showing a diffuse growth pattern. The ratio of each solid grade was determined each tumor area in middle-power view and was calculated for the entire tumor area. Then the predominant grades were determined for each PET. PET with large solid nests was defined if there was at least a large solid nest in the tumor, regardless of the overall solid grading. Grading was carried out by two observers independently.

Immunohistochemistry. Immunohistochemistry was done on the formalin-fixed, paraffin-embedded tissue sections using the avidin-biotin complex method as described previously (23). We used 4-μm-thick sections of representative blocks with antibodies against the

Table 1. Summary of patients' demographics

Variables	WHO-1 (n = 6)	WHO-2 (n = 14)	WHO-3 (n = 15)	WHO-4 (n = 2)	Total
Sex (male/female)	2/4	6/8	6/9	1/1	15/22
Median age (y)	58.5	55.5	52	30	55
Functional hormone syndrome*	0	2	2	0	4
Mean tumor size (cm)	1.2	3.6	6.4	10.0	4.7
Invasion to surrounding organs	0	0	10	2	12
Lymph node metastasis	0	0	13	2	15
Hematogenous metastasis [†]	0	1	8	1	10
Vascular invasion	0	4	13	2	19
Perineural invasion	0	3	10	2	15
Ki-67 labeling index >5	0	4	10	2	16
Follow-up					
Alive and well without disease	5	13	7	1	26
Alive with disease	0	0	3	0	3
Dead of disease	0	1	4	1	6
Dead of other cause	1	0	1	0	2

*Four patients showed the clinical manifestation associated with hypersecretion of insulin in two cases: glucagon in one and gastrin in another.
[†]Tumor metastasized to liver or other organs by hematogenous spreading before and/or after the surgical resection of PETs.

following: chromogranin A (poly; 1:500), synaptophysin (poly; 1:50), neuron-specific enolase (BBS/NC/VI-H14; 1:100), CD31 (JC/70A; 1:50), CD34 (QBEnd 10; 1:100), Factor VIII (poly; 1:1000), α -smooth muscle actin (α -SMA; 1A4; 1:50), and Ki-67 (MIB-1; 1:100) from DAKO (Glostrup, Denmark); CD56 (NCC-Lu-243; 1:50) from Nippon Kayaku (Tokyo, Japan); VEGF-A (poly; 1:100) from Santa Cruz Biotechnology (Santa Cruz, CA); and CXCL-12 (79018; 1:50) from R&D Systems, Inc. (Minneapolis, MN). As a brief description, the sections were deparaffinized and rehydrated. After blocking of endogenous peroxidase with methanol containing 0.3% H₂O₂, the sections were autoclaved at 121°C for 10 min in citrate buffer (10 mmol/L sodium citrate, pH 6) for antigen retrieval. After blocking with normal goat serum, the sections were reacted overnight with appropriately diluted primary antibodies. The sections were then reacted sequentially with biotin-conjugated anti-mouse immunoglobulin G antibodies (Vector Laboratories, Burlingame, CA) and Vectastain Elite ABC reagent (Vector Laboratories). For staining VEGF-A, the sections were boiled at 95°C for 10 min for antigen retrieval. Diaminobenzidine was used as the chromogen, and the nuclei were counterstained with hematoxylin. For semiquantitative assessments of the immunohistochemical results for VEGF-A and CXCL-12, cytoplasmic staining intensity and the proportion of positive tumor cells were recorded. A staining index (with a value of 0-9) was calculated as the product of staining intensity (0-3) and area of positive staining (0, <1%; 1, 1-10%; 2, 10-50%; 3, >50%; ref. 23). The upper quartile was used as the cutoff point. The Ki-67 labeling index was determined as described previously (23). Immunohistochemical double staining for CD34 and Ki-67 was also done as described previously (24). Initially, Ki-67 was stained and visualized with diaminobenzidine as a brown-colored chromogen, followed by detachment of antibodies; then secondary immunohistochemistry was done to detect CD34; and the reaction product was visualized with VIP as a purple-colored chromogen (Vector Laboratories).

Evaluation of i.t. MVD. For evaluation of i.t. MVD, microvessels were detected by morphologic observation and immunohistochemical labeling with the endothelial markers CD31, CD34, and Factor VIII. In our preliminary study, three different markers detected endothelial cells similarly. CD34 showed the strongest intensity among them and could detect endothelial cells easily, but sometimes, it labeled fibroblasts that could be easily distinguished from vascular endothelial cells by their histology. Factor VIII showed the weakest staining intensity among them. Then we used CD34 for MVD assay and CD31 for immunofluorescence double staining. All independent CD34-positive vessel structures were counted, irrespective of the presence of an identifiable lumen. For assessment of MVD, we used three different methods as follows. Average MVD (Av-MVD) was analyzed by selecting 10 randomized fields per tumor at a magnification of $\times 200$ (0.95 mm² per field), and the number of CD34-positive vessel structures in each field was counted. The mean number of vessels was then calculated after exclusion of the lowest and highest values measured (16). Hotspot MVD was assessed by a modification of the Weidner technique (21). The H&E-stained tissue sections were screened, and three areas with the most intense vascularization were selected at low magnification. We then counted CD34-positive vessels at a magnification of $\times 200$, and the average counts for the three fields were calculated. For solid area MVD (S-MVD), the H&E-stained tissue sections were screened, and we selected three areas showing the most solid growth pattern of tumor cells, which often contained large solid nests or a diffuse growth pattern. Then CD34-positive vessels at a magnification of $\times 200$ were counted in each corresponding area. The average counts of the three fields was calculated and defined as the S-MVD. Two observers, having no access to the patient data, evaluated independently MVD, morphometrical vessel characters, and proliferating endothelial cells described below. Their final value was the average of the value counted by the two observers. To assess intraobserver reproducibility, several tissue sections were counted thrice by each observer. To assess interobserver reproducibility, 10 data counted by each observer for the same tumor were compared (16).

Immunofluorescence double staining. Immunofluorescence double staining was done on 30- μ m-thick, formalin-fixed, paraffin-embedded tissue sections as described previously (24), with some modifications. All antibodies were diluted in 0.2% Triton X-100 and 5% skim milk in TBS-T. α -SMA antigens were stained by the CSA system (DAKO) with our modification, and then CD31 was stained with CSAII (DAKO). Reaction time for the primary and secondary antibodies was extended to overnight and 1 h, respectively. After reaction with biotin-conjugated tyramide solution, the sections were incubated with Texas Red-conjugated avidin (1:200) for 1 h at room temperature. After detaching the antibodies by acid treatment (100 mmol/L glycine/HCl, pH 2.2) for 2 h, the sections were stained with CD31 using CSAII according to the manufacturer's instructions with modifications. Just after reaction of the sections with FITC-conjugated tyramide, the sections were washed and mounted with Vectashield mounting medium (Vector Laboratories). Immunostained tissue sections were analyzed with a confocal microscope (LSM5 Pascal; Carl Zeiss Jena GmbH, Jena, Germany) equipped with a 15-mW Kr/Ar laser. The confocal files were saved, compiled, and fused to make three-dimensional pictures.

To estimate the branching frequency of blood vessels, 12 randomized fields were selected for each tumor at a magnification of $\times 200$. The distance of blood vessels between the closest two branches in each field was measured, and the mean length for each tumor was calculated, which we termed the unbranched vessel length. To estimate variability in the luminal diameter of blood vessels, 12 randomized fields were selected for each tumor at a magnification of $\times 400$. The maximum and minimum luminal diameters of blood vessels between the closest two branches in each field were measured, and the average of the difference in diameter was calculated. To evaluate abnormality of blood vessels showing irregular vessel wall shapes and distortion, i.t. vessels were divided into five categories: category 1 corresponded to regular vessels in normal islets of Langerhans, category 5 corresponded to the most severely changed vessels as shown in Fig. 4G to I, and categories 2 to 4 corresponded to vessels with mild to severe abnormalities between categories 1 and 5.

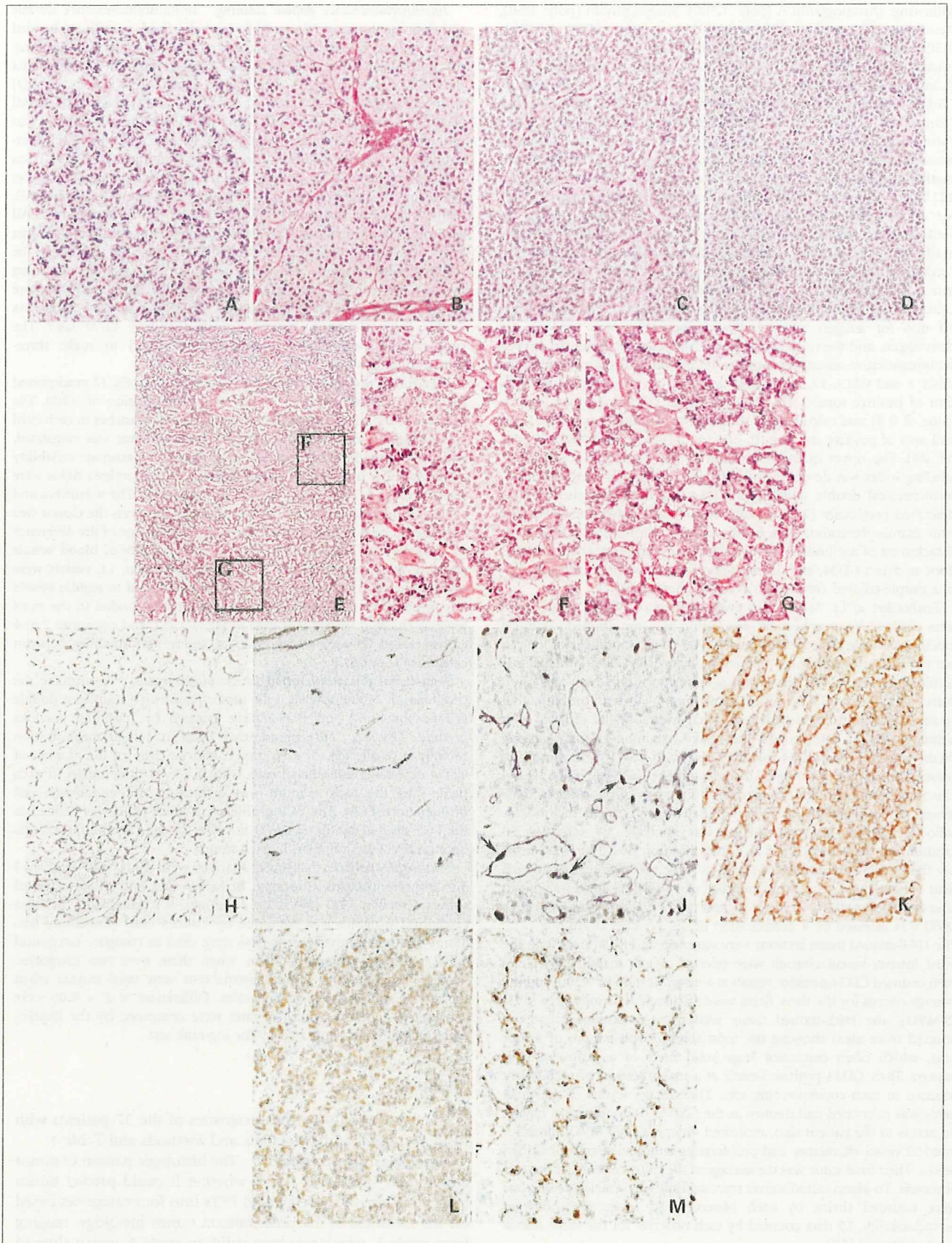
Endothelial cell proliferation in i.t. blood vessels. To evaluate the proliferation of endothelial cells, tumor tissues that had been double stained for Ki-67 and CD34 were assessed by modified previous methods (25, 26). Fifty randomized fields at a high magnification ($\times 400$) were selected for each tumor, and we counted the number of CD34-expressing endothelial cells with Ki-67-positive nuclei in each field, then the total amount was defined as the endothelial cell proliferation (ECP). The ECP proliferation index (EPI) was defined as the ECP divided by the Av-MVD that was assessed in the same fields because MVD was different in each tumor.

Statistical analysis. Statistical analyses were done with StatView-J 5.0 software (Abacus Concepts, Berkeley, CA) and SPSS statistical software version 12.0 (SPSS, Inc., Chicago, IL). Association between categorical variables was examined by Fisher's exact probability test. Mann-Whitney nonparametric tests were used to compare categorical with continuous tumor variables when there were two categories, whereas Kruskal-Wallis nonparametric tests were used instead when there were more than two categories. Differences at $P < 0.05$ were considered significant. Survival rates were computed by the Kaplan-Meier method and compared by the log-rank test.

Results

The clinicopathologic characteristics of the 37 patients with PETs are described in Materials and Methods and Table 1.

Histologic structural pattern. The histologic pattern of tumor growth was studied to clarify whether it could predict tumor behavior. Initially, we classified PETs into four categories based on the solidness of the predominant tumor histology, ranging from grade 1, which was least solid, to grade 4, which showed



the most solid and diffuse growth (Fig. 1A-D). Most of the PETs were classified as grade 1 (19 of 37; Table 2), which included tumors with a predominant histologic structure showing a thin trabecular, gyriform, or pseudoglandular pattern. All of the grade 3 PETs belonged to WHO-3, and grade 4 PETs belonged to WHO-4. There was no significant correlation between any of the grades and disease-free survival, but disease-free survival became closely correlated when grade 1 and 2 PETs were combined (Fig. 2A).

We then selected PETs that had a "large solid nest" defined as the presence of ≥ 11 tumor cells in the minor axis, independent of the overall tumor histologic pattern (Fig. 1E-G). Twenty PETs had large solid nests, including five grade 1 PETs, seven grade 2 PETs, and eight grade 3 and grade 4 PETs (Table 2). Interestingly, all the patients that suffered tumor recurrence had PETs with large solid nests, and all the patients without large solid nests remained disease-free. The presence of large solid nests was a significant factor correlated with disease-free survival (log-rank test, $P = 0.003$; Fig. 2B). The presence of large solid nests was significantly correlated with tumor size ($P = 0.008$), invasion to surrounding organs ($P = 0.002$), lymph node metastasis ($P = 0.018$), hematogenous metastasis ($P = 0.0006$), vascular invasion ($P = 0.0002$), and Ki-67 index ($P = 0.007$; Table S1).

MVD. The relationship between MVD and biological behavior in human PETs is controversial (16–18), probably as a result of how MVD is counted. To clarify whether MVD is related to tumor behavior and to select the best way to count MVD, we tried to measure MVD of PETs using three different counting methods (Materials and Methods; Fig. 1H and I): Av-MVD, hotspot MVD, and S-MVD. Av-MVD ranged from 59.4 to 423.5 vessels per field (mean, 189.1; median, 167.6); hotspot MVD ranged from 132.3 to 625.0 vessels per field (mean, 288.3; median, 268.0); and S-MVD ranged from 30.0 to 468.3 vessels per field (mean, 161.5; median, 132.3). Av-MVD and S-MVD decreased according to the progression of PETs by the WHO classification, and this was statistically significant (Kruskal-Wallis test: Av-MVD, $P = 0.010$; S-MVD, $P = 0.003$; Fig. 3A and Fig. S1). Hotspot MVD did not show apparent differences among the WHO classes ($P = 0.500$; Fig. S1). When all the PETs were divided into two groups based on median MVD, the high MVD group showed longer patient survival than the low MVD group (Fig. 3B and Fig. S1). The difference was clearer for S-MVD (log-rank test, $P = 0.002$), and the high S-MVD group included no patients with recurrent tumors. S-MVD was significantly correlated with tumor size ($P = 0.002$), invasion to surrounding organs ($P = 0.001$), lymph node metastasis ($P = 0.0006$), hematogenous metastasis ($P = 0.0004$), vascular invasion ($P < 0.0001$), perineural invasion ($P = 0.007$), and Ki-67 index ($P = 0.0002$; Table S1).

Vascular ECP. The dynamics of neoangiogenesis in PETs was assessed by ECP (Materials and Methods; Fig. 1J). ECP ranged from 0 to 26 (mean, 7.59; median, 7). Surprisingly, the ECP was higher in low S-MVD tumors ($P = 0.011$; Fig. 3C). EPI (Materials and Methods; range, 0.00–0.27; mean, 0.057;

Table 2. Relationship between histologic structural grades or tumors with large solid nests and WHO classification of pancreatic endocrine tumors

	Grade 1	Grade 2	Grade 3	Grade 4	Total cases
WHO-1	4 (1)	2 (2)	0	0	6 (3)
WHO-2	11 (2)*	3 (1)	0	0	14 (3)
WHO-3	4 (2)**	5 (4)*	6 (6)****	0	15 (12)
WHO-4	0	0	0	2 (2)*	2 (2)
Total	19 (5)	10 (7)	6 (6)	2 (2)	37 (20)

NOTE: The numbers of patients with PET having large solid nests are in parentheses.

n, number of asterisks () represent numbers of patients with PET recurrence.

median, 0.038) was also higher in PETs with low S-MVD and was significantly correlated with WHO classification (Kruskal-Wallis test, $P = 0.001$; Fig. 3D). When patients were divided into two groups by the median EPI, the high EPI group showed significantly shorter disease-free survival than the low EPI group (log-rank test, $P = 0.005$; Fig. 3E). EPI was significantly correlated with tumor size ($P < 0.0001$), invasion to surrounding organs ($P = 0.005$), lymph node metastasis ($P = 0.020$), hematogenous metastasis ($P = 0.003$), vascular invasion ($P < 0.0001$), and Ki-67 index ($P = 0.0008$; Table S1).

Vascular characteristics. We then analyzed the structures of blood vessels to determine whether blood vessels change to poorly formed vessels with multiple abnormalities, in association with tumor progression. We analyzed 9 PETs with high S-MVD and 13 PETs with low S-MVD that were available for immunofluorescence analysis using 30- μm -thick tissue sections stained for CD31 and α -SMA. There were fine mesh-like structures consisting of smooth, thin, and relatively regular vessels in tumors with high S-MVD (Figs. 1H and 4D-F). The rough structure of the vasculature in tumors with high S-MVD was similar to the vascular features of normal islets of Langerhans (Fig. 4A-C), although the vessels in the tumors were thick, and their detailed structures were irregular. In contrast, the vasculature in PETs with low S-MVD was less branched and relatively straight (Fig. 4J), consisting of thicker, more irregularly shaped and often distorted vessels (Figs. 1I, 4G-I and 4L). In high-power view, instead of mature branches, there were many very small and irregular buds on the vessels, which showed highly abnormal features (Fig. 4I). α -SMA-positive cells covered these irregular buds. The luminal diameter of vessels was more variable in PETs with low S-MVD than in PETs with high S-MVD (Fig. 4K). Almost all the i.t. blood vessels were covered by α -SMA-positive mural cells, although α -SMA-positive multiple layers were often observed in PETs with low S-MVD. These findings indicated that i.t. blood vessels in PETs with low S-MVD were poorly formed blood vessels with multiple abnormalities,

Fig. 1. A to D, histologic structural grading of PETs based on the degree of solid growth of tumor cells in the predominant architecture. Grade 1 tumor consists of small nests (A). Grade 2 tumor consists of moderate nests (B). Grade 3 tumor consists of large solid nests (C). Grade 4 tumor grows in a diffuse solid pattern (D). E to G, large solid nests. Tumor cells proliferate predominantly in a trabecular pattern and sometimes form large solid nests focally in low-power view (E). Middle-power view of large solid nests (F) and trabecular pattern (G). H to M, immunohistochemistry. CD34-labeled endothelial cells are detected in PET with high MVD (H) and in PET with low MVD (I) in low-power view. J, CD34 (purple) is expressed in vascular endothelial cells, and nuclei of proliferating cells are labeled by Ki-67 (brown) in high-power view. Arrows, proliferating endothelial cells. K, VEGF-A stained in cytoplasm of PET cells in middle-power view. CXCL-12 stained in PET cells (L) and blood vessels (M) in middle-power view.

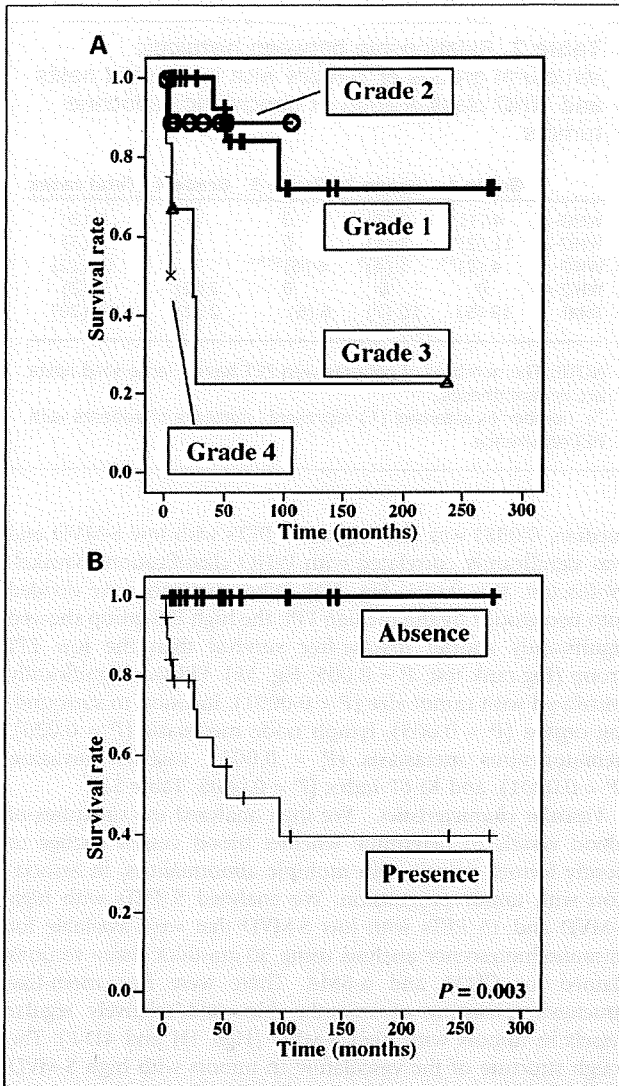


Fig. 2. Kaplan-Meier survival curves of the 37 patients with PETs. *A*, PETs are classified by predominant histological structures into four grades. There was no significant correlation between this classification and disease-free survival. *B*, PETs are divided by the presence or absence of large solid nests. Patients with PETs showing large solid nests had significantly shorter disease-free survival (log-rank test, $P = 0.003$).

whereas blood vessels in PETs with high S-MVD still had the characteristics of endocrine organs.

Expression of VEGF-A and CXCL-12 in PETs. To assess the angiogenic factors in PETs, we analyzed the expression of VEGF-A and CXCL-12 in tumor cells and i.t. blood vessels by immunohistochemistry (Fig. 1K-M). CXCL-12 is known to be a CXC chemokine involved in the recruitment of circulating endothelial progenitor cells from bone marrow to the target organs (27, 28). High expression of CXCL-12 in tumor cells was significantly correlated with high EPI ($P = 0.020$; Table 3) and low S-MVD ($P = 0.0006$; Table 3), although expression of CXCL-12 in i.t. blood vessels and VEGF-A expressed in tumor cells did not closely correlate with EPI and S-MVD (Table 3). High expression of VEGF-A in tumor cells was significantly correlated with high expression of CXCL-12 in i.t. blood vessels

($P < 0.0001$) but not to other clinicopathologic variables, including expression of CXCL-12 in tumor cells (Table 3). A high value of CXCL-12 in the tumor was significantly correlated with marked vascular invasion ($P = 0.0006$), the presence of hematogenous metastasis ($P = 0.006$), large tumor size ($P = 0.035$), a high Ki-67 index ($P = 0.006$), and the presence of large solid nests ($P = 0.018$). Furthermore, PETs having high amounts of CXCL-12 in the tumor cells were closely correlated with a shorter disease-free patient survival rate (log-rank test, $P = 0.018$; Fig. 3F).

Discussion

In this study, we found a new histologic marker for predicting the biological behavior of PETs (i.e., “the presence of focal large solid nests”), which is independent of the predominant histologic structure. Then we measured S-MVD and showed a close correlation between low MVD and an unfavorable prognosis in PETs. Paradoxically, i.t. vessels of PETs with a high MVD showed low EPI and vice versa. Morphometric analysis showed that blood vessels in PETs with low MVD were more poorly formed and had more irregular and abnormal features, whereas blood vessels in PETs with high MVD showed relatively regular mesh-like features similar to vessels in normal islets of Langerhans. These findings imply that a high MVD seems to be a characteristic of blood vessels in islets of Langerhans, and that EPI can be a hallmark of angiogenic activity in tumor-associated blood vessels in PETs. Our data also suggest that EPI and S-MVD are predictors of the biological behavior of PETs. We analyzed angiogenic factors in PETs and found that high EPI and low MVD were significantly correlated with high expression of CXCL-12 in tumor cells but not with the expression of CXCL-12 in i.t. blood vessels and VEGF-A. Combined with the data for the relationship between CXCL-12 and other variables, it is suggested that CXCL-12 produced in tumor cells is involved in the angiogenesis of tumor-associated vessels and hematogenous spread as well as proliferation of tumor cells and thus may contribute to the aggressiveness of PETs. CXCL-12 is the first molecule to be highlighted as a possible angiogenic factor playing important roles in the neoangiogenesis of PETs. Thus, we have provided novel data on the prognostic features of tumor architecture and tumor-associated angiogenesis in PETs.

In contrast to the predominant histologic structures, the presence of focal large solid nests delineated PETs with aggressive behavior. Even in grade 1 and 2 PETs, patients with large solid nests had significantly shorter disease-free survival than patients without them ($P = 0.024$). Interestingly, metastatic PETs showed almost the same histologic architecture as the original pancreatic tumors and were not occupied by tumor cells with solid growth. These findings suggest that tumor cells in large solid nests are not more progressed or more malignant than their origin, and that the presence of large solid nests represents the potential for tumor malignancy.

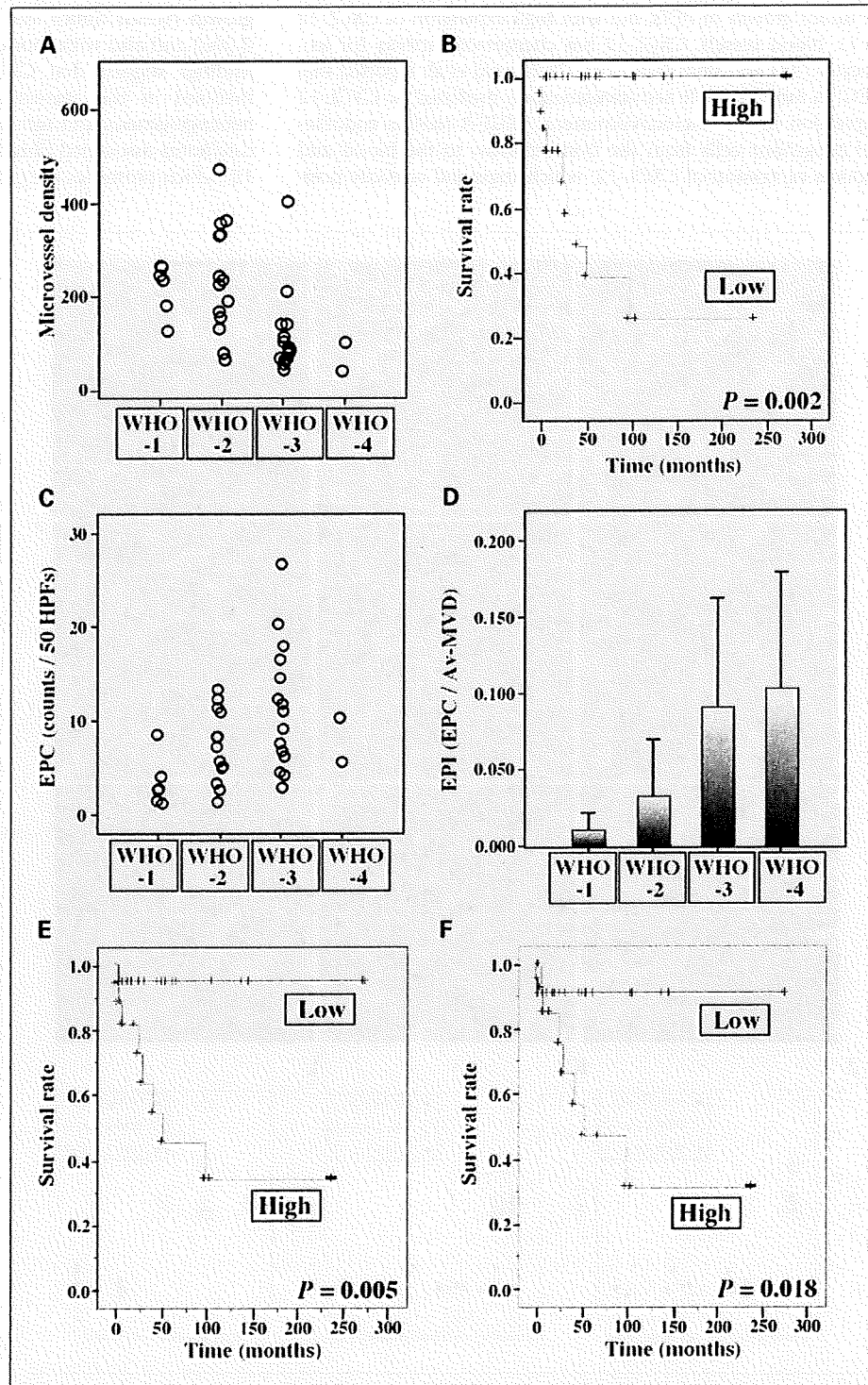
By comparing three methods for evaluation of MVD, we found that the best variable for predicting the representative biological characteristics of PETs was S-MVD. This seems reasonable because in PETs, we showed that a focal tumor structure showing the most solid growth represents the behavior of the tumor as a whole. Morphometric analysis also showed that irregularity and abnormality of i.t. blood vessels were associated with tumor growth pattern where the vessels were present. These findings

imply that tumor architecture is closely correlated with local vessel formation, and that tumor cells and blood vessels seem to be a pair of components within a single structure.

Our results indicate that EPI and MVD can be prognostic variables in patients with PETs. Abnormal tumor-associated blood vessels tend to grow rapidly (10), consistent with the fact that PETs with more poorly formed blood vessels have a high

EPI. EPI is also significantly correlated with hematogenous spread (vascular invasion, $P < 0.0001$; hematogenous metastasis, $P = 0.003$) and survival ($P = 0.005$) in PETs. Recently, similar results were indicated in the other tumor by Stefansson et al. That is, increased vascular proliferation was associated with aggressive features of tumors and was an independent prognostic factor in endometrial carcinoma (26).

Fig. 3. A, C, and D, relationship between vascular index and WHO classification. B, E, and F, Kaplan-Meier survival curves of 37 patients with PETs. A, S-MVD significantly decreased according to progression of PETs in terms of the WHO classification (Kruskal-Wallis test, $P = 0.003$). B, patients were divided into two groups by median S-MVD. The high S-MVD group showed significantly longer survival than the low S-MVD group (log-rank test, $P = 0.002$). C, EPC significantly increased according to progression of PETs in terms of the WHO classification (Kruskal-Wallis test, $P = 0.019$). D, EPI significantly increased according to progression of PETs in terms of the WHO classification (Kruskal-Wallis test, $P = 0.001$). E, patients were divided into two groups by median EPI. The high EPI group showed significantly shorter survival than the low EPI group (log-rank test, $P = 0.005$). F, patients were divided into two groups by the quartile value of CXCL-12 expressed in the tumor cells. Patients with PETs showing high expression of CXCL-12 in the tumor cells had significantly shorter survival than those whose tumors showed low expression (log-rank test, $P = 0.018$).



What kinds of molecules are involved in tumor-associated angiogenesis in PETs? It has been reported that in many kinds of cancers VEGF produced in tumor cells accelerates tumor-associated angiogenesis, leading to tumor growth and a high frequency of hematogenous tumor cell spread (14). VEGF-A expression in PETs is reported to be not closely correlated with MVD (16, 18) or to be closely correlated with high MVD (17). In our series, there was no close correlation of VEGF-A expression with growth of blood vessels, hematogenous spread, or tumor growth in PETs, but with high expression of CXCL-12 in i.t. blood vessels. CXCL-12 has chemotactic activity for leukocytes (28) and stem cells (29). Grunewald et al. reported that VEGF-A induces adult neovascularization mediated by CXCL-12 expression in the microenvironment. VEGF-A recruits endothelial progenitor cells from the bone marrow to the blood and induces expression of CXCL-12, which traps and correctly posi-

tions endothelial progenitor cells around growing vessels in tissues (27). Our study suggested that VEGF-A induced the expression of CXCL-12 in tumor vessels, although such events did not lead to tumor-associated neoangiogenesis in PETs. In contrast, high EPI was closely correlated with high CXCL-12 produced in tumor cells ($P = 0.020$). High expression of CXCL-12 in tumor cells was also positively correlated with variables of hematogenous tumor spread (versus vascular invasion, $P = 0.0006$; versus hematogenous metastasis, $P = 0.006$) and tumor growth (versus tumor size, $P = 0.035$; versus Ki-67 index, $P = 0.006$) and also with shorter patient survival ($P = 0.018$). These findings suggest that CXCL-12 produced in tumor cells is involved in the aggressive features of tumor mediated by neoangiogenesis and tumor growth. Orimo et al. reported that carcinoma-associated fibroblasts in breast cancer secrete CXCL-12, which promotes the growth of the tumor cells both directly

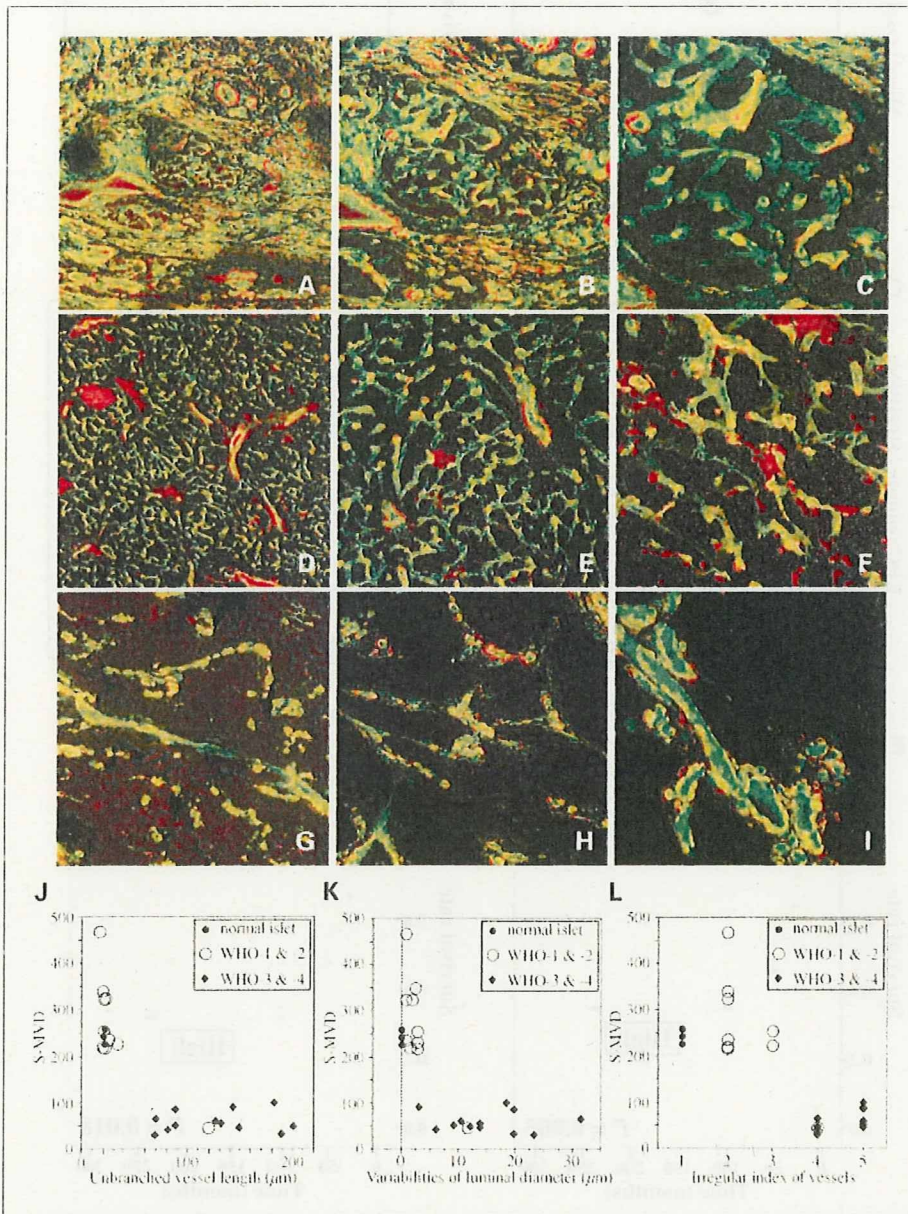


Fig. 4. Characterization of tumor-associated blood vessels in double immunofluorescence examination of CD31 (green) and α -SMA (red) using 30- μ m-thick sections. Normal islet of Langerhans in low-power (A), middle-power (B), and high-power (C) view. PET with high S-MVD in low-power (D), middle-power (E), and high-power (F) view. PET with low S-MVD in low-power (G), middle-power (H), and high-power (I) view. J to L, morphometric analyses of PETs. I.t. blood vessels were examined for unbranched vessel length (J), variability of luminal diameter (K), and vessel irregularity (L).

Table 3. Relationship between clinicopathologic variables and VEGF-A or CXCL-12

Variables	n	VEGF-A			CXCL-12 in tumor cells			CXCL-12 in blood vessels		
		High (n = 19)	Low (n = 18)	P	High (n = 19)	Low (n = 18)	P	High (n = 19)	Low (n = 18)	P
Age (y)										
≤55	19	8	11	NS	8	11	NS	8	11	NS
>55	18	10	8		7	11		11	7	
Sex										
Female	22	13	9	NS	10	12	NS	13	9	NS
Male	15	5	10		5	10		6	9	
Functional hormone syndrome										
Absence	33	16	17	NS	14	19	NS	17	16	NS
Presence	4	2	2		1	3		2	2	
Tumor size (cm)										
<2	13	3	10	0.038	2	11	0.035	4	9	NS
≥2	24	15	9		13	11		15	9	
Invasion to surrounding organs										
Absence	25	12	13	NS	7	18	NS	15	10	NS
Presence	12	6	6		8	4		4	8	
Lymph node metastasis										
Absence	22	8	14	NS	6	16	NS	11	11	NS
Presence	15	10	5		9	6		8	7	
Hematogenous metastasis*										
Absence	27	12	15	NS	7	20	0.006	13	14	NS
Presence	10	6	4		8	2		6	4	
Vascular invasion										
Absence	18	6	12	NS	2	16	0.0006	9	9	NS
Presence	19	12	7		13	6		10	9	
Perineural invasion										
Absence	22	10	12	NS	7	15	NS	12	10	NS
Presence	15	8	7		8	7		7	8	
Ki-67 labeling index										
≤5	21	8	13	NS	4	17	0.006	9	12	NS
>5	16	10	6		11	5		10	6	
Histologic structural grades										
1 + 2	29	15	14	NS	10	19	NS	18	11	0.019
3 + 4	8	3	5		5	3		1	7	
Large solid nests										
Absence	17	7	10	NS	3	14	0.018	9	8	NS
Presence	20	11	9		12	8		10	10	
S-MVD										
High	18	7	11	NS	2	16	0.0006	10	8	NS
Low	19	11	8		13	6		9	10	
EPI										
High	18	11	7	NS	11	7	0.020	10	8	NS
Low	19	7	12		4	15		9	10	
VEGF-A										
High	18				10	8	NS	16	2	<0.0001
Low	19				5	14		3	16	
CXCL-12 in tumor cells										
High	15	10	5	NS				8	7	NS
Low	22	8	14					11	11	
CXCL-12 in vessels										
High	19	16	3	<0.0001	8	11	NS			
Low	18	2	16		7	11				

Abbreviation: NS, not significant.

*Tumor metastasized to liver or other organs by hematogenous spreading before and/or after the surgical resection of PETs.

and indirectly, and promotes neoangiogenesis by recruiting endothelial progenitor cells (30). Finally, high expression of CXCL-12 in tumor cells had a close correlation with the presence of large solid nests ($P = 0.018$). It is possible that CXCL-12 produced by tumor cells may mediate the formation of focal solid structures by a pair of solid growing tumor cells and their surrounding tumor-associated blood vessels with highly abnormal features. Furthermore, it is suggested that interrupting the angiogenic

pathway mediated by CXCL-12 may provide a novel and efficient antiangiogenesis strategy for the treatment of PETs.

Acknowledgments

We thank Drs. Kazuaki Shimada, Yoshihiro Sakamoto, Hidenori Ojima, and Hiroki Ochiai for useful discussions and Kaoru Onozato, Yuko Yamauchi, Fumi Kaiya-Toshioka, Ayaka Miura, and Rie Itoh for their technical advice.

References

1. DeLellis RA, Lloyd RV, Heitz PU, Eng C. World Health Organization classification of tumours. Pathology and genetics of tumours of endocrine organs. Lyon: IARC Press; 2004. p. 175–208.
2. Solcia E, Capella C, Klöppel G. Tumors of the pancreas. Atlas of tumor pathology, 3rd series, fascicle 20. Washington (DC): Armed Forces Institute of Pathology; 1997.
3. Maderia I, Terris B, Voss M, et al. Prognostic factors in patients with endocrine tumours of the duodeno-pancreatic area. *Gut* 1998;43:422–7.
4. Hochwald SN, Zee S, Conlon KC, et al. Prognostic factors in pancreatic endocrine neoplasms: an analysis of 136 cases with a proposal for low-grade and intermediate-grade groups. *J Clin Oncol* 2002;20:2633–42.
5. Jorda M, Ghorab Z, Fernandez G, Nassiri M, Hanly A, Nadjji M. Low nuclear proliferative activity is associated with nonmetastatic islet cell tumors. *Arch Pathol Lab Med* 2003;127:196–9.
6. Deshpande V, Castillo CF, Muzikansky A, et al. Cytokeratin 19 is a powerful predictor of survival in pancreatic endocrine tumors. *Am J Surg Pathol* 2004;28:1145–53.
7. Goto A, Niki T, Terada Y, Fukushima J, Fukayama M. Prevalence of CD99 protein expression in pancreatic endocrine tumors (PETs). *Histopathology* 2004;45:384–92.
8. Hanahan D, Folkman J. Patterns and emerging mechanisms of the angiogenic switch during tumorigenesis. *Cell* 1996;86:353–64.
9. Lopez T, Hanahan D. Elevated levels of IGF-1 receptor convey invasive and metastatic capability in a mouse model of pancreatic islet tumorigenesis. *Cancer Cell* 2002;1:339–53.
10. Jain RK. Molecular regulation of vessel maturation. *Nat Med* 2003;9:685–93.
11. Morikawa S, Baluk P, Kaidoh T, et al. Abnormalities in pericytes on blood vessels and endothelial sprouts in tumors. *Am J Pathol* 2002;160:985–1000.
12. Hashizume H, Baluk P, Morikawa S, et al. Openings between defective endothelial cells explain tumor vessel leakiness. *Am J Pathol* 2000;156:1363–80.
13. Ellis LM, Fidler IJ. Tumor angiogenesis. In: Mendelsohn J, Howley PM, Israel MA, et al. editors. The molecular basis of cancer. 2nd ed. Philadelphia: Saunders; 2001. p. 173–85.
14. Carmeliet P, Jain RK. Angiogenesis in cancer and other diseases. *Nature* 2000;407:249–57.
15. Poon RTP, Ng IOL, Lau C, et al. Tumor microvessel density as a predictor of recurrence after resection of hepatocellular carcinoma: a prospective study. *J Clin Oncol* 2002;20:1775–85.
16. Marion-Audibert AM, Barel C, Gouysse G, et al. Low microvessel density is an unfavorable histoprognostic factor in pancreatic endocrine tumors. *Gastroenterology* 2003;125:1094–104.
17. Couvelard A, O'Toole D, Turley H, et al. Microvascular density and hypoxia-inducible factor pathway in pancreatic endocrine tumours: negative correlation of microvascular density and VEGF expression with tumour progression. *Br J Cancer* 2005;92:94–101.
18. La Rosa S, Uccella S, Finzi G, Alvarello L, Sessa F, Capella C. Localization of vascular endothelial growth factor and its receptors in digestive endocrine tumors: correlation with microvessel density and clinicopathologic features. *Hum Pathol* 2003;34:18–27.
19. Tan G, Cioc AM, Perez-Montiel D, Ellison EC, Frankel WL. Microvascular density does not correlate with histopathology and outcome in neuroendocrine tumors of the pancreas. *Appl Immunohistochem Mol Morphol* 2004;12:31–5.
20. Folkman J. Clinical applications of research on angiogenesis. *N Engl J Med* 1995;333:1757–63.
21. Weidner N. Tumoural vascularity as a prognostic factor in cancer patients: the evidence continues to grow. *J Pathol* 1998;184:119–22.
22. Weidner N, Semple JP, Welch WR, Folkman J. Tumor angiogenesis and metastasis - correlation in invasive breast carcinoma. *N Engl J Med* 1991;324:1–8.
23. Takahashi Y, Hiraoka N, Onozato K, et al. Solid-pseudopapillary neoplasms of the pancreas in men and women: do they differ? *Virchows Arch* 2006;448:561–9.
24. Hiraoka N, Onozato K, Kosuge T, Hirohashi S. Prevalence of FOXP3⁺ regulatory T cells increases during the progression of pancreatic ductal adenocarcinoma and its premalignant lesions. *Clin Cancer Res* 2006;12:5423–34.
25. Eberhard A, Kahlert S, Goede V, et al. Heterogeneity of angiogenesis and blood vessel maturation in human tumors: implications for antiangiogenic tumor therapies. *Cancer Res* 2000;60:1388–93.
26. Stefansson IM, Salvesen HB, Akslen LA. Vascular proliferation is important for clinical progress of endometrial cancer. *Cancer Res* 2006;66:3303–9.
27. Grunewald M, Avraham I, Dor Y, et al. VEGF-induced adult neovascularization: recruitment, retention, and role of accessory cells. *Cell* 2006;124:175–89.
28. Bluel CC, Farzan M, Choe H, et al. The lymphocyte chemoattractant SDF-1 is a ligand for LESTR/fusin and blocks HIV-1 entry. *Nature* 1996;382:829–33.
29. Peled A, Petit I, Kollet O, et al. Dependence of human stem cell engraftment and repopulation of NOD/SCID mice on CXCR4. *Science* 1999;283:845–8.
30. Orimo A, Gupta PB, Sgroi DC, et al. Stromal fibroblasts present in invasive human breast carcinomas promote tumor growth and angiogenesis through elevated SDF-1/CXCL12 secretion. *Cell* 2005;121:335–48.